BUMPLESS TRANSFER FOR SWITCHED SYSTEMS

LAURA MARCELA SALAZAR CRUZ

PONTIFICIA UNIVERSIDAD JAVERIANA
FACULTAD DE INGENIERÍA
DEPARTAMENTO DE ELECTRÓNICA
BOGOTÁ DC, 2012

BUMPLESS TRANSFER FOR SWITCHED SYSTEMS

LAURA MARCELA SALAZAR CRUZ

TRABAJO DE INVESTIGACIÓN
MAESTRÍA EN INGENIERÍA ELECTRÓNICA

DIRECTOR:
ING. DIEGO ALEJANDRO PATIÑO GUEVARA, Ph.D.

PONTIFICIA UNIVERSIDAD JAVERIANA
FACULTAD DE INGENIERÍA
DEPARTAMENTO DE ELECTRÓNICA
BOGOTÁ DC, 2012

PONTIFICIA UNIVERSIDAD JAVERIANA

FACULTAD DE INGENIERÍA

MAESTRÍA EN INGENIERÍA ELECTRÓNICA

RECTOR MAGNÍFICO: P. JOAQUIN EMILIO SÁNCHEZ GARCÍA S.J

DECANO ACADÉMICO: ING. LUIS DAVID PRIETO, Ph.D.

DECANO DEL MEDIO UNIVERSITARIO: P. SERGIO BERNAL RESTREPO S.J

DIRECTOR DE MAESTRÍA: ING. CARLOS PARRA, Ph.D

DIRECTOR DE PROYECTO: ING. DIEGO ALEJANDRO PATIÑO GUEVARA, Ph.D.

Bumpless Transfer for Switched Systems

Laura M. Salazar

Department of Engineering

Pontificia Universidad Javeriana

A thesis submitted for the degree of

Master in Electronic Engineering

June 2012

Contents

List of Figures

Nota de Advertencia

"La Universidad no se hace responsable por los conceptos emitidos por sus alumnos en sus trabajos de tesis. Solo velará por que no se publique nada contrario al dogma y a la moral católica y por que las tesis no contengan ataques personales contra persona alguna, antes bien se vea en ellas el anhelo de buscar la verdad y la justicia".

Artículo 23 de la Resolución N° 13, del 6 de julio de 1946, por la cual se reglamenta lo concerniente a Tesis y Exámenes de Grado en la Pontificia Universidad Javeriana.

Reminder Note

"This university is not responsible for the concepts issued by its students in their grade project. This university will only ensure that they do not publish anything contrary to the catholic dogma and that this work does not contain personal attacks or polemics. Rather than that, it is seen in them the desire to seek truth and justice".

Article 23 in the resolution issued in 6th of july of 1946, which regulates the issues concerning the thesis and grade exams in the Pontificia Universidad Javeriana.

Chapter 1

Introduction

1.1 Context

Control theory is an interdisciplinary area of engineering and mathematics that seeks to model and manipulate the behavior of dynamical systems. Depending on the variables involved, dynamical systems can be classified as continuous, discrete or hybrid (involving continuous and discrete dynamics), and therefore it must be controlled using appropriate techniques to the corresponding domain.

The main characteristics used to describe the dynamics of a system are stability, observability, controllability and linearity. The latter refers to if the system response is linear around a given operating point and it is the main criterion for simplification of the proposed models.

The successful design of linear control systems can be attributed in part to the ease of implementation of linear controllers and the associated mathematical formulation of the theory of linear systems. However, due to the nonlinearity of real systems, most linear controllers must be designed around a specific operating point. As it must be ensured that the system is successfully controlled throughout its operating range, it is more common to design a linear controller, each in a different operating point and switch among them. Therefore, it is necessary to implement strategies to control systems at several operating points automatically.

The hybrid dynamical systems, especially switched dynamical systems are an alternative for solving control problems with multiple operating points, since by combining continuous and discrete dynamics, one can characterize the behavior of the system's discrete state changes as necessary for the switching between the controllers of continuous dynamics, and increase the operating range of the control system design.

However, while this strategy avoids the design of more complex (nonlinear) controllers, when switching between a finite set of controllers, the control signal may have undesirable transients or discontinuities when the active controller (online) and the new controller (offline, which will switch) have different outputs at the switching instant, so that the switching process introduces a nonlinearity in the loop causing transients and discontinuities which could eventually affect adversely the system response [1]. The removal of these transients is known as "Bumpless Transfer".

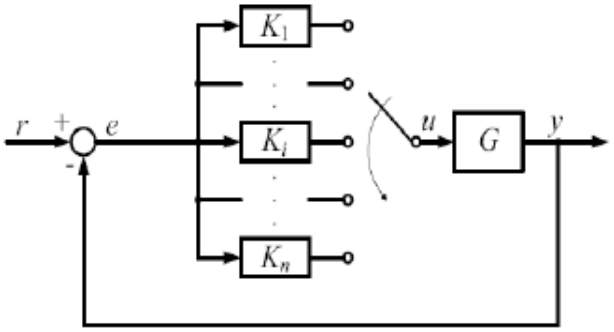

Figure 1.1: Switched Control System. [2]

At present, there are several applications of the switched control systems, such as temperature control systems, automobiles, regulated sources and level control systems. However, in most industrial applications, there are saturations when performing the switching between controllers because the limits of the actuators do not accept these discontinuities, which leads to the modification of the dynamic performance of the system and it is not possible to ensure its stability [5]. Therefore, it is necessary to eliminate unwanted behaviors in the control signal and to ensure bumpless transfer when switching between controllers.

1.2 Motivation

The web winding system, shown in figure 1.2, is an example of a plant that requires the transportation of material at a desired voltage and speed, ensuring that the tape does not break or deteriorate. This system is structured with the following components: two DC motors with optical encoders (w_1, w_2), connected to each one of the reels, an optical encoder coupled to one of the pulleys or axes (w_3), a dancer arm system, whose rotation axis is fixed to a linear potentiometer (θ), a radius measuring system of one of the reels, estimating the radius from the voltage of a potentiometer (r) which is coupled to a nylon rod, and is located on the belt, and finally, a set of mechanical parts essential to the operation of the web winding system [7].

Figure 1.2: Web Winding System. [7]

For this system, three MIMO LTI models of fourth order were estimated for different intervals of the radius: for the first model, the data were taken for a radius between $0.025m > r > 0.0167m$ (R1) for the second model, $0.0167m > r > 0.0084m$ (R2) and for the third model, $0.0084m > r > 0.0001m$ (R3) [7].

Currently, a LPV technique is used on the web winding system [7], which is responsible for performing a balancing of the three controllers (one for each model) by estimating the radious. However, if it is desired to switch controllers, the discontinuities and bumps obtained in the control signal adversely alter the system, and they can deteriorate or damage the tapes. Therefore, it is required to implement a strategy to achieve bumpless transfer when switching among the three models with their corresponding $\mathcal{H}_\infty$ controllers which were designed to reduce the effect of external disturbances.

1.3 Problem Overview

To achieve bumpless transfer on switched systems, it must be ensured that there are not discontinuities or transients in the control signal when switching between different controllers designed with respect to a specified operating point.

When the outputs of the controllers are different, the control signal can present perturbations in a time near the switching instant. The aim is to ensure continuity in the control signal and to smooth transitions in the time immediately after the switching time.

It is desired to find a technique that allows bumpless transfer, and that ensures an optimality criterion and stability, with respect to the initialization of the offline controller states to those of the online controller. Therefore, it is wanted to find a method that eliminates discontinuities in the control signal based on the techniques used in [1], [2], [3] and apply it by simulation on the web winding system of the control laboratory.

The following activities were performed in this work:

- Control law as an algorithm to avoid bumps and discontinuities.
- Simulation of the control law on the web winding system of the control laboratory.
- Stability analysis of the switched system with the control law.

In this project, it is given a brief description of the bumpless transfer on the web winding system of the control laboratory and $\mathcal{H}_\infty$ controllers are designed via LMI's for the system, using the theorems given in [6]. Then, the simulations are subsequently displayed and finally some conclusions about the work obtained and future work are given.

1.4 Bibliography Review

A description of the most popular strategies to achieve bumpless transfer are found in [1], [2], [3] and [5]. In this work we use the techniques described in [1] , [2] , [3].

Among the most popular strategies to achieve bumpless transfer, are:

The high gain approach [17], attempts to force the offline control signal to be identical to the online control signal through a large gain that is placed in a feedback loop around the online controller. However, if the system has right half plane zeros, including zeros at infinity, the gain in the loop can not be increased indefinitely. This could make this approach ineffective.

The Hanus conditioning scheme [18], attempts to initialize the offline controller states to those of the online controller to partially inverting the offline controller to synthesize a realizable reference, but can not be generalized, as many controllers lack a direct feedback term.

The LQ (linear-quadratic) bumpless transfer scheme [1], minimizes a cost function in a linear quadratic context, which involve two weighting matrices to add flexibility to the design. A static feedback gain is synthesized to drive the offline controller in such a way that, at the time of transfer between the online and offline controllers, the transients produced by this switching are minimal.

The steady-state bumpless transfer under controller uncertainty using the state/output feedback topology [3] is a method that retains the convenience of the Turner and Walker design [1]. It introduces a novel state/output feedback bumpless transfer topology that employs the nominal state of the offline controller and, through the use of an additional controller/model mismatch compensator, also the offline controller output.

The bumpless transfer for switching adaptive controllers [2], is a method based on the decomposition of a controller in slow and fast dynamics that is inspired by an adaptive PID control (fast mode: derivative, slow mode: integrator). It can be performed without precise knowledge of the plant at the switching instants. By restarting the states of fast and slow modes at the switching instants, continuity in the control signal is ensured and transients after switching are avoided.

The bumpless transfer for discrete time switched systems [5], proposes an additional controller which is activated at the switching instant to reduce the discontinuity of the control signal, guaranteeing the performance of the output of the plant.

However, although some solutions have been raised in specific cases, it has not been formulated yet a strategy to solve the general problem of bumpless transfer on switched systems. We need to find a control law that minimizes the discontinuities and bumps, and that ensures internal stability.

1.5 Objectives

This project has the following general and specific objectives:

1.5.1 General objective

Find a strategy to solve the problem of bumpless transfer for switched systems, by eliminating discontinuities in the control signals.

1.5.2 Specific objectives

- Implement and evaluate methods to achieve bumpless transfer in switched systems.
- Find an algorithm that allows bumpless transfer, based on optimal control theory.
- Implement the proposed strategy by simulation on the web winding system of the control laboratory.
- Compare the performance with that obtained with the LPV control technique used on the web winding system of the control laboratory, by simulation.

1.6 Contribution and Organization

The contribution of this work is an application of bumpless transfer techniques in switched systems, minimizing discontinuities on the control signal. Also, $\mathcal{H}_\infty$ controllers of a low order were designed. One of the main interest of this thesis is that stability was evaluated for different bumpless methods and an example of an unstable bumpless

transfer method was found. The document is organized in 6 chapters and is structured as follows:

Chapter 1

Chapter 1 is an introduction to bumpless transfer. A review of the problem and the bibliography is presented. Some of the main problems that are important are also described here.

Chapter 2

Chapter 2 presents an introduction of the basic principles used in this thesis. The formal definitions and representations of bumpless transfer, $\mathcal{H}_\infty$ controllers and stability are presented. Also, the web winding system model is presented.

Chapter 3

Chapter 3 presents the linear quadratic bumpless transfer, bumpless transfer for adaptive switching controls and the steady-state bumpless transfer under controller uncertainty using the state/output feedback topology strategies on discrete time systems. Also, an one step predictive controller is developed.

Chapter 4

Chapter 4 presents the system's stability analysis. The system's closed loop matrices were found when applying some bumpless transfer methods and stability was evaluated using multiple Lyapunov functions. Also, an example of an unstable method is exposed.

Chapter 5

Chapter 5 presents the application, simulation and results of the bumpless transfer strategies applied on the web winding system, the elimination of the discontinuities on the control signals and the principal results on stability. At the end of the chapter some analysis of the obtained results are presented.

Chapter 6

Chapter 6 presents the conclusions of the work, some new perspectives and open problems to be treated and a few problems encountered during the performance of the work.

Chapter 2

Basic Principles

Bumpless transfer arises in many cases of practical interest as switching between dynamic controllers that does not induce bumps in the plant output. One such case is switching between several linear controllers, each one of them designed to provide the desired closed-loop performance in the neighborhood of its operating point, to cover the entire operating range of a nonlinear plant [4]. An example of this is the web winding system of the control laboratory that does not function correctly when switching and therefore, it is required to implement a strategy to achieve bumpless transfer.

On the other hand, bumpless transfer techniques may lead to stability problems. If it is assumed that the online and offline controllers are stabilizing for the plant, around a certain operating point, the stability of the closed-loop system around this operating point, without switching occurring, is guaranteed. However, nothing can be concluded in general about the stability of the overall system when arbitrary switching occurs [1].

In this chapter, an introduction of the bumpless transfer techniques applied on the web winding system is given. In addition, a $\mathcal{H}_\infty$ controller design procedure via LMIs is presented. This was used to implement faster and simpler controllers than the ones design in [7] for this system. Finally, it is given an introduction on stability of switched systems and a stability condition through multiple Lyapunov functions.

2.1 Bumpless Transfer

In this section, the bumpless transfer techniques ([1], [2] and [3]) applied on the web winding system are introduced.

2.1.1 Linear Quadratic Bumpless Transfer

Assume that the state vector is $x \in \mathbb{R}^n$, the control signal is $u \in \mathbb{R}^m$, the error vector (the difference between the reference and the plant output) is $\tilde{e} \in \mathbb{R}^p$, the output of the plant is $y \in \mathbb{R}^p$, and the reference signal is $r \in \mathbb{R}^p$. All other vectors and matrices shall be assumed to be of compatible dimensions.

A static feedback matrix F is derived in order to drive the *offline* controller in such a way that, at the time of transfer between *online* and *offline* controllers the transients produced by this switching are minimal. This scheme is shown in Fig. 2.1.

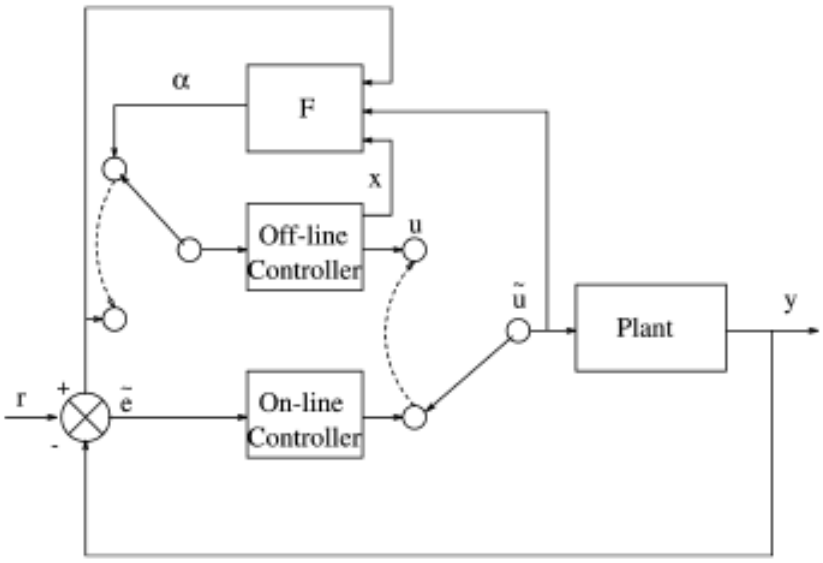

Figure 2.1: Bumpless Transfer Scheme. [1]

To achieve a 'minimal' amount of transient behavior during switching we shall min-

imize a quadratic cost function. Firstly, at the time of switching, it is desirable that the *online* and *offline* controllers produce control signals which are as close to each other as possible, in order to reduce the magnitude of the discontinuity which occurs during transfer. Secondly, we must also take into account the signals driving the controllers. It is desirable to avoid a large difference between these signals because, in order to maintain good tracking, the signal driving the *offline* controller will be switched to the error signal. That is, after switching the *offline* controller becomes the current *online* controller [1]. This situation is described diagrammatically in Fig. (2.1).

This technique provides a convenient computational setting for bumpless transfer involving high order linear finite dimensional time invariant controllers. However, in several important MIMO industrial applications, this technique is found to provide an incomplete convergence of the output of the offline controller to that of the online controller and produce a pronounced nonvanishing error between the outputs of these controllers [3].

A closer examination of the possible causes of this offline/online controller output error reveals that it arises due to the following reason: the design in [1] assumes that the bumpless transfer operator is provided with the true state of the offline controller and the input to it, and that these two quantities fully characterize the offline controller output.

Under this assumption, the availability of the offline controller output, when its input and state are used, is completely redundant and has nothing to contribute to the bumpless transfer, therefore these designs consciously discard the offline controller output data in the full state configurations.

2.1.2 The steady-state bumpless transfer under controller uncertainty

The linear quadratic bumpless transfer technique that was just introduced can be extendable to synthesize the matrix F in the state/output feedback topology of Fig. 2.2.

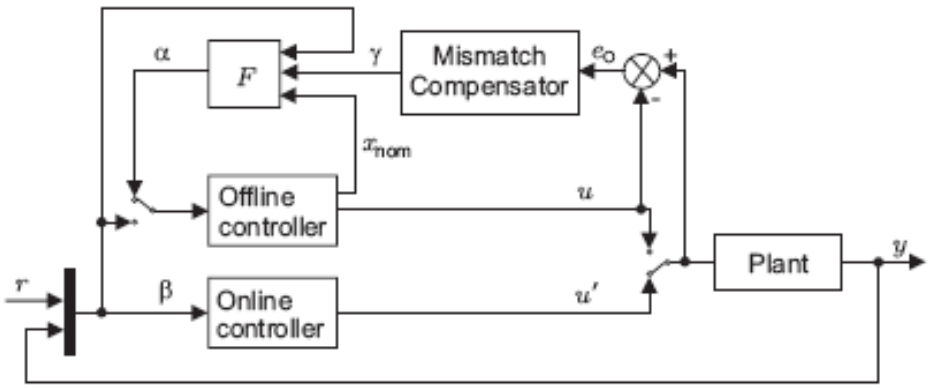

Figure 2.2: State/Output feedback bumpless transfer scheme. [3]

Redefining $z_e(t)$ and $z_u(t)$ as $z_e(t) = \alpha(t) - \beta(t)$ and $z_u(t) = u(t) - u'(t)$ respectively, the performance criterion becomes applicable to the topology of Fig. 2.2 and the feedback matrix can be calculated [3].

The topology of the design in [1] uses the online controller input and output feedback and, the offline controller state feedback. In reference to the latter, it is called the state feedback topology. The topology presented in Fig. 2.2 is characterized by the simultaneous utilization of the state and the output of the offline controller, and it is called the output feedback topology.

The transfer operator in this topology combines essentially two distinct groups of controllers, the state feedback and the output feedback ones. This nested architecture allows to retain the steady-state LQ design of [1] for the inner loop, while employing a simple integral control law for the outer loop [3].

2.1.3 Bumpless Transfer for Adaptive Switching Controls

Consider the switching control system as shown in Fig. 2.3. The system includes a plant and a set of controllers

$$K = \{K_1, ..., K_i, ..., K_n\} \ (i = 1, 2, ..., n) \tag{2.1}$$

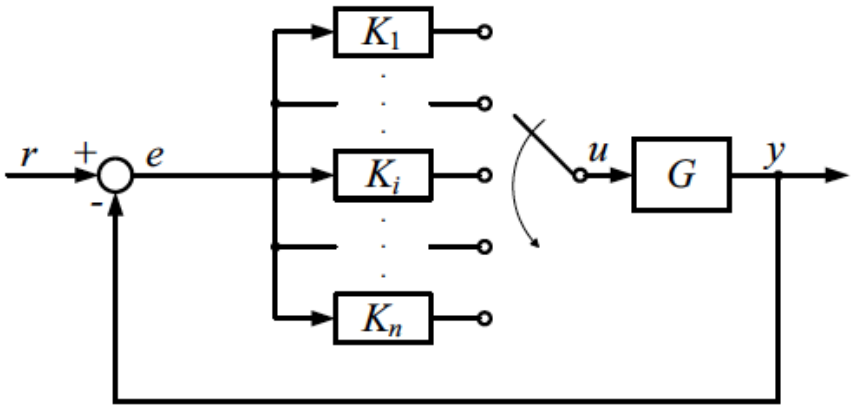

Figure 2.3: Switching control system. [2]

When controller K_i is in the feedback loop, then this controller is said to be *online*, and the other controllers are said to be *offline*.

Bumpless Transfer method based on slow-fast decomposition of the controller is inspired by an adaptive PID controller. It is a special case of the controller which has fast modes (the differentiator) and slow modes (the integrator). Generalizing the PID controller case, the method decomposes the original controllers into the fast modes controllers and the slow modes controllers.

By appropriately re-initializing the states of the slow and fast modes at switching times, it can be ensured that not only will the controller output be continuous, but also that it avoid fast transient bumps after switching [2].

The disadvantage with this method is that the re-initialization of the states of the

slow and fast modes only assures (in some case) no jumps at the switching instant, which do not guarantee there will be no transient problems with infinite combinations of the controller states (no matter on the value of the control signal). This is the difference between a method that only acts at the switching time [2] and a method that acts on the long term and that really tries to condition the controller state for having the best behavior [1].

2.2 $\mathcal{H}_\infty$ Controllers

In this section, an introduction to $\mathcal{H}_\infty$ control and dynamic $\mathcal{H}_\infty$ controller design for discrete time systems via LMIs is given.

This procedure was implemented on the web winding system in order to obtain faster and simpler controllers (4 states) that the ones designed in [9] (10 states).

2.2.1 $\mathcal{H}_\infty$ Control

Consider the system described by the block diagram where the plant G and controller K

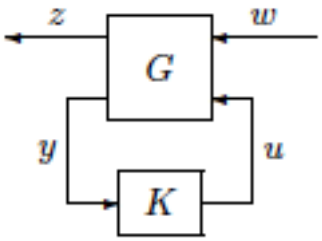

Figure 2.4: System [16]

are assumed to be real rational and proper. It will be assumed that state-space models of G and K are available and that their realizations are assumed to be stabilizable and detectable. Recall again that a controller is said to be *admissible* if it internally stabilizes the system. Clearly, stability is the most basic requirement for a practical system to work. Hence any sensible controller has to be admissible [16].

Optimal $\mathcal{H}_\infty$ Control

Find all admissible controllers $K(s)$ such that $||T_{zw}||_\infty$ is minimized.

Subptimal $\mathcal{H}_\infty$ Control

Given $\gamma > 0$, find all admissible controllers $K(s)$, if there are any, such that $||T_{zw}||_\infty < \gamma$.

For more information, see appendix A.

2.2.2 $\mathcal{H}_\infty$ Controller Design for Discrete Time Systems

Consider the following discrete time linear system

$$x(k+1) = Ax(k) + B_w w(x) + B_u u(k) \tag{2.2}$$
$$z(k) = C_z x(k) + D_{zw} w(k) + D_{zu} u(k) \tag{2.3}$$
$$y(k) = C_y x(k) + D_{yw} w(k) \tag{2.4}$$

$T_{wz}(\zeta)$ denotes the transfer function from the input w to the output z.

For a dynamic output feedback problem with respect to the full order linear dynamic controller given by

$$x_c(k+1) = A_c x_c(k) + B_c y(k) \tag{2.5}$$
$$u(k) = C_c x_c(k) + D_c y(k) \tag{2.6}$$

Where the controller state is $x_c \in \mathbb{R}_c^n$, and connecting the controller with the system, the closed loop state space representation is given by

$$\tilde{x}(k+1) = \tilde{A}\tilde{x}(k) + \tilde{B}w(k) \tag{2.7}$$
$$z(k) = \tilde{C}\tilde{x}(k) + \tilde{D}w(k) \tag{2.8}$$

with the following closed loop matrices

$$\tilde{A} = \begin{bmatrix} A + B_u D_c C_y & B_u C_c \\ B_c C_y & A_c \end{bmatrix} \tag{2.9}$$

$$\tilde{B} = \begin{bmatrix} B_w + B_u D_c D_{yw} \\ B_c D_{yw} \end{bmatrix} \tag{2.10}$$

$$\tilde{C} = \begin{bmatrix} C_z + D_{zu} D_c C_y & D_{zu} C_c \end{bmatrix} \tag{2.11}$$

$$\tilde{D} = \begin{bmatrix} D_{zw} + D_{zu} D_c D_{yw} \end{bmatrix} \tag{2.12}$$

$\mathcal{H}_\infty$ controllers of the same number of states of the system can be found using the results shown on theorem 2.2.1.

Theorem 2.2.1. ***(output feedback $\mathcal{H}_\infty$)*** *All controllers in the form (2.5)-(2.6) such that the inequality $\|T_{wz}\|_\infty^2 < \mu$ holds are parametrized by the LMI*

$$\begin{bmatrix} P_H & J_H & AX_H + B_u L_H & A + B_u R_H C_y & B_w + B_u R_H D_{yw} & 0 \\ J_H' & H_H & Q_H & Y_H A + F_H C_y & Y_H B_w + F_H D_{yw} & 0 \\ (AX_H + B_u L_H)' & Q_H' & X_H + X_H' - P_H & I + S_H' - J_H & 0 & X_H' C_z' + L_H' D_{zu}' \\ (A + B_u R_H C_y)' & (Y_H A + F_H C_y)' & (I + S_H' - J_H)' & Y_H + Y_H' - H_H & 0 & C_z' + C_y' R_H' D_{zu}' \\ (B_w + B_u R_H D_{yw})' & (Y_H B_w + F_H D_{yw})' & 0 & 0 & I & D_{zw}' + D_{yw} R_H' D_{zu}' \\ 0 & 0 & (X_H' C_z' + L_H' D_{zu}')' & (C_z' + C_y' R_H' D_{zu}')' & (D_{zw}' + D_{yw}' R_H' D_{zu}')' & \mu I \end{bmatrix} > 0 \tag{2.13}$$

Where the matrices X_H, L_H, Y_H, F_H, Q_H, R_H, S_H, J_H and the symmetric matrices P_H and H_H are the variables and $(')$ indicates transposition.

The proof of this theorem can be found in [6].

Given matrices X_H, L_H, Y_H, F_H, Q_H, R_H, S_H, J_H from this theorem, a feasible controller $\mathcal{H}_\infty$ is obtained by choosing U_H and V_H nonsingular such that $V_H U_H = S_H - Y_H X_H$. In this case, U_H was taken as the identity and $V_H = S_H - Y_H X_H$. And calculating [6]:

$$D_c = R_H \tag{2.14}$$

$$C_c = (L_H - R_H C_y X_H) U_H^{-1} \tag{2.15}$$

$$B_c = V_H^{-1} (F_H - Y_H B_u R_H) \tag{2.16}$$

$$A_c = V_H^{-1} [Q_H - Y_H (A + B_u D_c C_y) X_H - V_H B_c C_y X_H - Y_H B_u C_c U_H] U_H^{-1} \tag{2.17}$$

This LMI can be solved using Sedumi-Yalmip [10] or the linear matrix inequalities toolbox in Matlab.

2.3 Stability of Switched Systems

An important problem related to switched systems is the stability criteria. As mentioned before, bumpless transfer techniques may lead to stability problems because by implementing these techniques nothing can be concluded in general about the stability of the overall system when arbitrary switching occurs.

The concept of stability remains from the linear systems. It is a property assigned to a system and describes the quality to return to it is equilibrium point when the system is disturbed [12], [13]. In this section, a few background of stability of switched systems is presented.

2.3.1 Stability of Hybrid Systems

The main problems around stability of switched systems are:

- Find stability conditions such that hybrid system is stable.
- Given the switching law, determinate if the hybrid system is stable.
- Create a switching law that makes the hybrid system stable.

A switched system is *global uniform asymptotically stable* GUAS (see (2.5)(a)). if there exists a positive constant δ and β function such that for the sequence s (where s is the switching law) with $x(0) \leq \delta$ it follows

$$|x(t)| \leq \beta(\|x(0)\|, t) \forall t \geq 0 \tag{2.18}$$

If the β function is of the form $\beta(r, s) = cre^{\lambda s}$, for some $c, \lambda > 0$, and equation (2.18) is satisfied, the system is called *global uniform exponentially stable* GUES [14] (see Fig. 2.5(b)). Stability for a hybrid system can be studied from two perspectives. Independent from the switching signal s so in this case the common Lyapunov function is an useful alternative, or dependent of the switching signal s and for this case a piecewise Lyapunov function is more convenient.

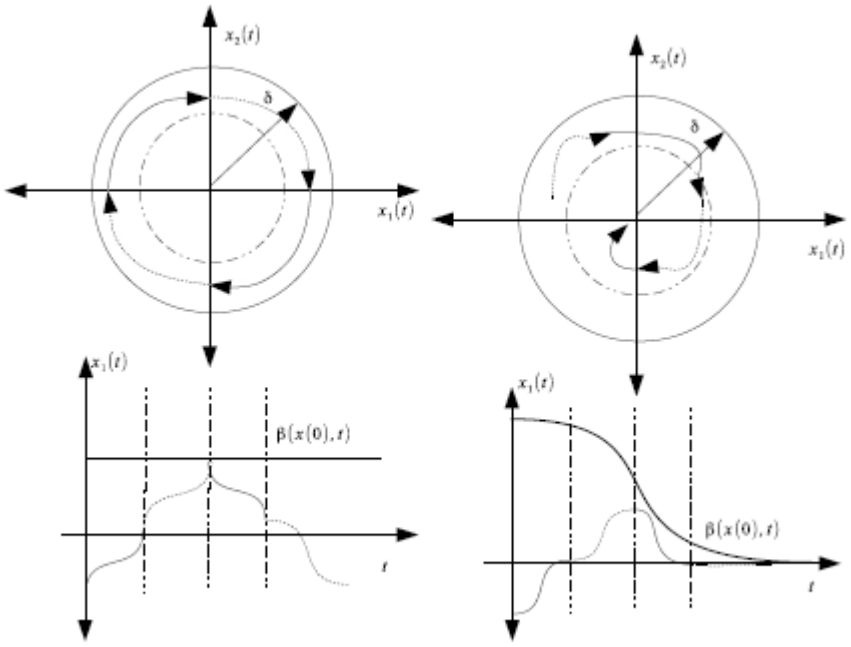

Figure 2.5: Stability for hybrid systems. [11]

The Lyapunov approach has a formal definition for non-linear systems shown in [13], [14]. An hybrid system of the following form:

$$\dot{x}(t) = A_i x(t), i = 1, 2, ..., q \tag{2.19}$$

Where $A_i \in \mathbb{R}^{n \times n}$, describes the dynamic of the system. The stability of the hybrid system can be analyzed with the help of a function $V(x)$.

2.3.2 Multiple Lyapunov Function

Stability for a system can also be obtained by making the Lyapunov function a piecewise affine function with certain features. These are families of piecewise continuous functions that concatenated produce a single Lyapunov function. For a linear time

invariant system, it is suggested a set of Lyapunov functions as it follows.

$$V(x) = \{V_i(x) = x^T P_i x, i \in Q\} \tag{2.20}$$

Equation (2.20) must satisfy the following conditions:

- $V_i(x) = x^T P_i x$ is a positive definite function $\forall x \neq 0$ and $V(0) = 0$.
- $\frac{dV_i(x)}{dt} \leq 0, \forall i \in Q$

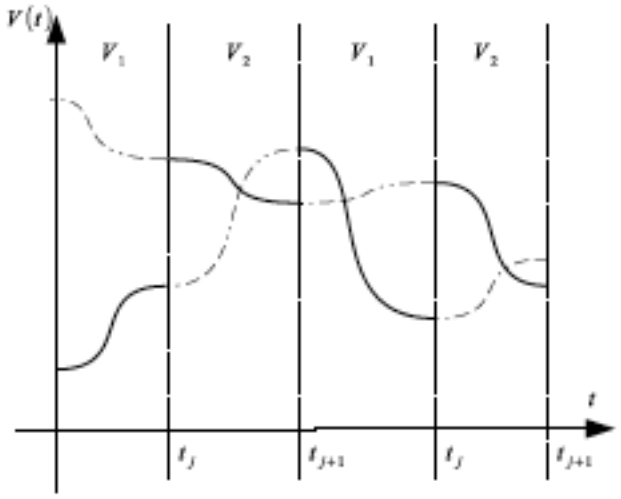

Figure 2.6: Multiple Lyapunov Function. [15]

Figure 2.6 shows an stable hybrid dynamical system. The stability of the system is based on the decay of the Lyapunov function (2.20) at any successive times, the system is switched according to a sequence s [13]. In the case of linear time invariant systems, suppose a Lyapunov function like (2.20). The following result can be obtained [14], [15]:

Theorem 2.3.1. *A switched linear system (2.18) is GUES for an arbitrary sequence s if and only if the following linear matrix inequalities hold for some positive definite matrix Q:*

$$A_i^T P_i + P_j A_i < -Q, \forall i, j = 1, 2, ..., q \tag{2.21}$$
$$(i, j) \in Q \times Q \tag{2.22}$$

Remark 2.3.1. ***(Discrete Time)*** *In case of a discrete time system the linear matrix inequality to hold is:*

$$A_i^T P_j A_i - P_i < -Q, \forall i, j \in Q \times Q \tag{2.23}$$

One of the main advantages of the multiple Lyapunov function is that it is a less conservative principle based on finding different functions for each mode of the hybrid dynamical system [14], [15].

Chapter 3

Bumpless Transfer

In this chapter, the bumpless transfer strategies applied on the web winding system are presented: linear quadratic bumpless transfer, bumpless transfer for adaptive switching controls and the steady-state bumpless transfer under controller uncertainty using the state/output feedback topology. Also, an one step predictive controller is developed in order to predict the behavior of the output signals (found by applying the bumpless transfer strategies) at the switching instants, and to choose the better control according to an optimality condition.

3.1 Linear Quadratic Bumpless Transfer on Discrete Time Systems

Suppose that the system has 2 controllers and that the first controller is *online* and it is described by the difference equations:

$$x_c(k+1) = A_c x(k) + B_c \tilde{e}(k) \tag{3.1}$$

$$\tilde{u}(k) = C_c x(k) + D_c \tilde{e}(k) \tag{3.2}$$

and that the *offline* controller is described by the difference equations:

$$x_c^2(k+1) = A_c^2 x(k) + B_c^2 \alpha(k) \tag{3.3}$$

$$u(k) = C_c^2 x(k) + D_c^2 \alpha(k) \tag{3.4}$$

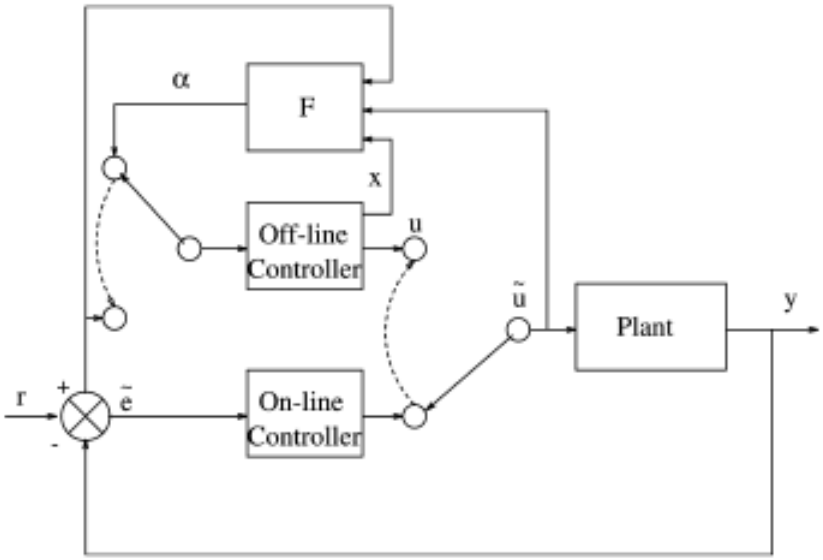

Figure 3.1: Bumpless Transfer Scheme. [1]

In order to minimize the difference between the *online* and *offline* control signals and also the difference between the signals driving the controllers: α, the signal produced by the 'subcontroller' F, and the control error $\tilde{e}$ in the LQ context, we have to minimize J, [1].

$$J = \frac{1}{2}\sum_{0}^{T-1}\left[z_u(k)'W_u z_u(k) + z_e(k)'W_e z_e(k)\right] + \frac{1}{2}z_u(T)'P_T z_u(T) \tag{3.5}$$

where

$$z_u(k) = u(k) - \tilde{u}(k) \tag{3.6}$$
$$z_e(k) = \alpha(k) - \tilde{e}(k) \tag{3.7}$$
$$z_u(T) = u(T) - \tilde{u}(T) \tag{3.8}$$

and where ($'$) indicates transposition, $\tilde{u}(k)$ and $\tilde{e}(k)$ are the *online* control signal and error signal, respectively; $u(k)$ is the *offline* control signal; $\alpha(k)$ is the signal produced by the feedback gain which drives the *offline* controller. W_u and W_e are constant

positive-definite weighting matrices of appropriate dimensions which are used to adapt the design as required. $z_u(k)$ and $z_e(k)$ are the error signals between the control signals and the signals driving the controllers, respectively.

Finally, $z_u(T) = u(T) - \tilde{u}(T)$ is the difference between the two control signals at the terminal time T, (which will most commonly be taken as infinity), and P_T is the positive semi-definite terminal weighting matrix.

Substituting (3.4) in (3.5) we can write

$$J = \frac{1}{2}\sum_{0}^{T-1}\Big[(C_c^2 x_c^2(k) + D_c^2\alpha(k) - u(\tilde{k}))'W_u(C_c^2 x_c^2(k) + D_c^2\alpha(k) - \tilde{u}(k))+\Big]$$
$$[+(\alpha(k) - \tilde{e}(k))'W_e(\alpha(k) - \tilde{e}(k))] + \frac{1}{2}z_u(T)'P_T z_u(T)$$

Applying a Lagrange multiplier, $\lambda(k) \in R^n$, we have

$$\tilde{J} = \frac{1}{2}\sum_{0}^{T-1} H(k) - \lambda'(k+1)x_c^2(k+1) + \Phi(T) \tag{3.9}$$

where $\Phi(T) = \frac{1}{2}z_u(T)'P_T z_u(T)$ and the Hamiltonian is defined as

$$H = \frac{1}{2}\{(C_c^2 x_c^2(k) + D_c^2\alpha(k) - \tilde{u}(k))'W_u(C_c^2 x_c^2(k) + D_c^2\alpha(k) - \tilde{u}(k))+$$
$$(\alpha(k) - \tilde{e}(k))'W_e(\alpha(k) - \tilde{e}(k))\} + \lambda'(k+1)(A_c^2 x_c^2(k) + B_c^2\alpha(k))$$

The first order necessary conditions for a minimum are given as

$$x_c^2(k+1) = \frac{\partial H(k)}{\partial\lambda(k+1)} \tag{3.10}$$
$$\lambda(k+1) = \frac{\partial H(k)}{x_c^2(k)} \tag{3.11}$$
$$0 = \frac{\partial H(k)}{\partial\alpha(k)} \tag{3.12}$$
$$\lambda(N) = \frac{\partial\Phi}{\partial x_c^2(N)} \tag{3.13}$$

Where (3.10) and (3.11) constitute the *state* x_c^2 and *co-state* λ equations respectively, where the co-state equation is a differential equation that has to be solved from the terminal condition, (3.13). Equation (3.12) is often referred as the *stationary condition*.

Solving these equations, it yields the following expression for F, [1]

$$\alpha(k) = \Delta \begin{bmatrix} (D_c^{2'} W_u C_c^2)' \\ B_c^2 \\ -(D_c^{2'} W_u)' \\ -W_e \end{bmatrix} \begin{bmatrix} x_c^2(k) \\ \lambda(k+1) \\ \tilde{u}(k) \\ \tilde{e}(k) \end{bmatrix} \tag{3.14}$$

where the adjoint equation is given by

$$\lambda(k+1) = \Pi(k+1) x_c^2(k+1) - g(k+1) \tag{3.15}$$

$\Pi(k+1)$ is the solution to the discrete-time Ricatti equation given by

$$\hat{A}'(I - \Pi(k+1)\hat{B})^{-1}\Pi(k+1)\hat{A} - \Pi(k) + \hat{C} = 0 \tag{3.16}$$

and $g(k+1)$ is the solution to the difference equation

$$g(k) = -\hat{A}'(I - \Pi(k+1)\hat{B})^{-1} g(k+1) \tag{3.17}$$

which are solved subject to the boundary conditions

$$\Pi(T) = (I - C_c^{2'} P_T D_c^2 \Delta B_c^{2'})^{-1} (C_c^{2'} P_T C_c^2 + C_c^{2\prime} P_T D_c^2 \Delta D_c^{2'} W_u C_c^2) \tag{3.18}$$

$$g(T) = (I - C_c^{2'} P_T D_c^2 \Delta B_c^{2'})^{-1} \begin{bmatrix} -(C_c^{2'} P_T D_c^2 \Delta D_c^{2'} W_u + C_c^{2'} P_T)' \\ -(C_c^{2'} P_T D_c^2 \Delta W_e) \end{bmatrix} \begin{bmatrix} \tilde{u}(T) \\ \tilde{e}(T) \end{bmatrix} \tag{3.19}$$

If $\hat{A}$, $\hat{B}$ and $\sqrt{\hat{C}}$ are stablisable and detectable, and $\Pi(T) \geq 0$, then the solution of the Riccati equation converges to a constant value in the infinite horizon: a value identical to the solution of the discrete algebraic Ricatti equation. (the proof can be found in [1]). Thus in the infinite horizon, F is given by

$$\alpha(k) = F \begin{bmatrix} x_c^2(k) \\ \tilde{u}(k) \\ \tilde{e}(k) \end{bmatrix} \tag{3.20}$$

$$F = \begin{bmatrix} F_x \\ F_u \\ F_e \end{bmatrix} \tag{3.21}$$

$$= (I - \Delta B_c^{2'} \Pi B_c^2)^{-1} \Delta \begin{bmatrix} (D_c^{2'} W_u C_c^2 + B_c^{2'} \Pi A_c^2)' \\ -(D_c^{2'} W_u + B_c^{2'} (I - M)^{-1} \hat{U})' \\ -(W_e + B_c^{2'} (I - M)^{-1} \hat{E})' \end{bmatrix} \tag{3.22}$$

Where

$$\Delta = -(D_c^{2'} W_u D_c^2 + W_e)^{-1} \tag{3.23}$$

$$\hat{A} = A_c^2 + B_c^2 \Delta D_c^{2'} W_u C_c^2 \tag{3.24}$$

$$\tilde{B} = B_c^2 \Delta B_c^{2'} \tag{3.25}$$

$$\tilde{C} = C_c^{2'} W_u C_c^2 + C_c^{2'} W_u D_c^2 \Delta D_c^{2'} W_u C_c^2 \tag{3.26}$$

$$M = \hat{A}'(I - \Pi \hat{B})^{-1} \tag{3.27}$$

$$\hat{U} = M \Pi B_c^2 \Delta D_c^{2'} W_u + C_c'^2 W_u + C_c^{2'} W_u D_c^2 \Delta D_c^{2'} W_u \tag{3.28}$$

$$\hat{E} = M \Pi B_c^2 \Delta W_e + C_c^{2'} W_u D_c^2 \Delta W_e \tag{3.29}$$

and Π is the stabilizing solution to the discrete-time algebraic Riccati equation:

$$\hat{A}'(I - \Pi \hat{B})^{-1} \Pi \hat{A} - \Pi + \hat{C} = 0 \tag{3.30}$$

which can also be written as

$$-\Pi + \hat{A}' \Pi \hat{A} - \hat{A}' \Pi B_c^2 (B_c'^2 \Pi B_c^2 + \Delta^{-1})^{-1} B_c^{2'} \Pi \hat{A} + \hat{C} = 0 \tag{3.31}$$

The solution to this Riccati equation corresponds to the stationary solution and can be found using the function 'Dare' in matlab.

3.2 Steady-State Bumpless Transfer Under Controller Uncertainty Using the State/Output Feedback Topology

The linear quadratic bumpless transfer technique that was just introduced, can be extendable to synthesize the matrix F in the state/output feedback topology of Fig. 3.2

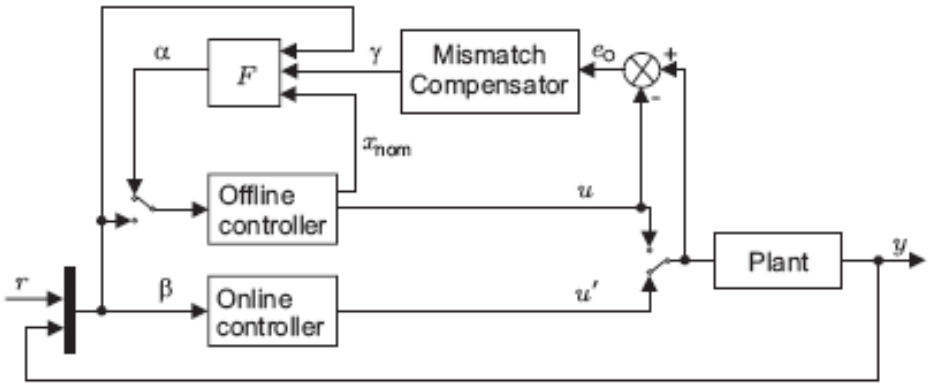

Figure 3.2: State/Output feedback bumpless transfer scheme. [3]

The transfer operator in this topology is seen to combine two distinct transfer operators in a nested configuration: the inner one, F, and the outer one, the mismatch compensator, forming the state and the output feedback loops, respectively. The inner operator F is designed to stabilize the offline controller and the outer mismatch compensator then drives the offline controller output to converge to the online controller output $\tilde{u}$. After the attainment of the latter, the switch at the input side of the offline controller turns to connect signal β to the offline controller. At the same time, the switch at the offline controller output side turns to disconnect online controller output $\tilde{u}$ from the plant input and connect the offline controller output u to the plant input, completing the bumpless transfer. This configuration permits retaining the infinite horizon LQ design of [1] for the inner loop, while employing, under certain conditions, a simple integral control law for the outer loop [4].

Mismatch Compensator Structure

The mismatch compensator design is carried out using the offline controller model. Assuming stable online controller operation, signals $\tilde{u}$ and β in Fig. 3.2 can be treated as bounded external inputs to the subsystem that generates signal α driving the offline controller output u. Based on this observation, the subsystem with no offline controller uncertainty can be represented by a nested loop configuration shown in Fig. 3.3. In this figure K and G denote the matrix transfer functions of the boxed subsystems.

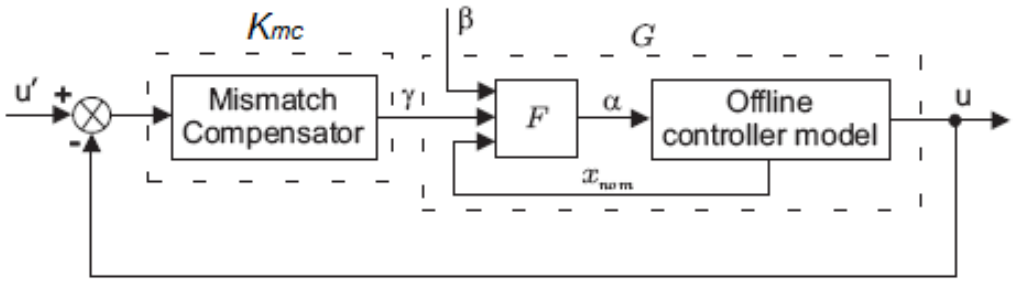

Figure 3.3: Nominal offline controller subsystem. [3]

The bumpless transfer performance requirement for the design of the mismatch compensator K_{mc} s to ensure that the closed loop provides convergence of u onto constant reference input, $\tilde{u}$, sufficiently fast for the application of interest, under constant output disturbance. Therefore, K_{mc} is simply selected as a bank of integral (I) controllers [3], as shown in Fig. 3.4, where $k_{int_i, i=1,\ldots,m}$, are the tuning knobs and m is the dimension of the controller output vector, which is the number of control signals.

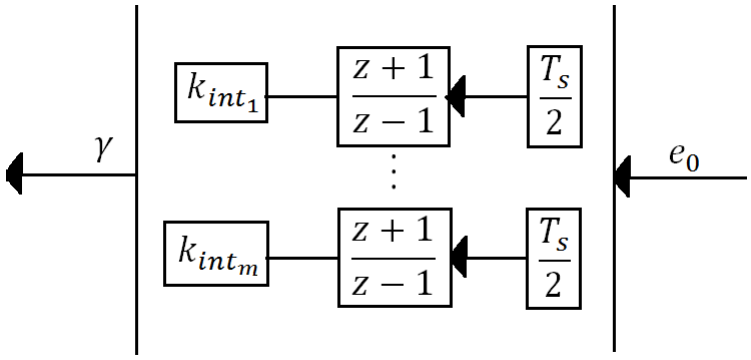

Figure 3.4: Internal model based controller/model mismatch compensator

3.3 Bumpless Transfer for Adaptive Switching Controls

As shown in Fig. 3.5, the input of the plant is $u(k)$ and the output is $y(k)$. Controller input is $e(k) = r(k) - y(k)$ where $r(k)$ is a reference signal.

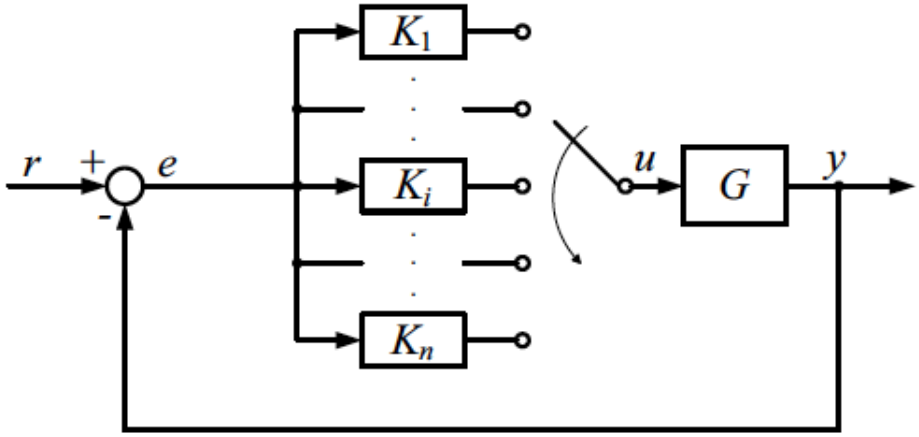

Figure 3.5: Switching control system. [2]

Switching Control System

Assuming that the *i-th* controller K_i is *online*, it has the state-space realization

$$x_c(k+1) = A_c^i x_i(k) + B_c^i e(k) \tag{3.32}$$

$$y_{K_i}(k) = C_c^i x_i(k) + D_c^i e(k) \tag{3.33}$$

where e is the controller input and y_{K_i} is the output.

$$K_i(s) = \left[\frac{A_c^i | B_c^i}{C_c^i | D_c^i}\right] \tag{3.34}$$

We are interested in the situation in which the *online* controller is switched from K_i to K_j at the instant k, so that

$$\begin{cases} y_{K_i} & for\ k < k^* \\ y_{K_j} & for\ k \geq k^* \end{cases} \tag{3.35}$$

Since the controller output y_{K_i} is replaced by y_{K_j} at the switching instant k^*, the control signal u can have bumps if y_{K_i} and y_{K_j} have different values [2].

The objective of bumpless transfer is to ensure continuity in the control signal and to smooth bumpy transients at, and immediately following, the switching instant.

Slow-fast decomposition

Consider that the controllers K_i $(i = 1, 2, ..., n)$ can be additively decomposed into slow and fast parts as follows:

$$K_i(s) = K_{islow}(s) + K_{ifast}(s) \tag{3.36}$$

with respective minimal realizations

$$K_{islow}(s) = \left[\frac{A_{cs}^i | B_{cs}^i}{C_{cs}^i | D_{cs}^i}\right] \tag{3.37}$$

$$K_{ifast}(s) = \left[\frac{A_{cf}^i | B_{cf}^i}{C_{cf}^i | D_{cf}^i}\right] \tag{3.38}$$

The poles of $K_{slow}(s)$ are of smaller magnitude than the poles of $K_{fast}(s)$

$$|\lambda_i(A_{cs})| \leq |\lambda_j(A_{cf})| \ \forall i, j \tag{3.39}$$

Then, the state-space realization of the *i-th* controller K_i is

$$x_c^i(k+1) = A_{cs}^i x_{cs}^i(k) + A_{cf}^i x_{cf}^i(k) + (B_{cs}^i + B_{cf}^i)e(k) \tag{3.40}$$

$$y_{K_i}(k) = C_{cs}^i x_{cs}^i(k) + C_{cf}^i x_{cf}^i(k) + (D_{cs}^i + D_{cf}^i)e(k) \tag{3.41}$$

A switching controller with slow-fast decomposition (3.36) is said to perform a bumpless transfer if, whenever controller is switched, the new controller state is reset so as to satisfy both of the following two conditions [2]:

1. The control input signal $u(k)$ is continuous at k^* whenever $r(t) \in C^0$.

2. The state of fast part of controller $K_{fast}(s)$ is reset to zero at k^*.

Assumption 1. For each candidate controller K_i, the slow part K_{islow} in (3.37) and (3.38) has at least $m = dim(u)$ states.

The Assumption 1 is sufficient to allow the state of the slow controller $K_{islow}(s)$ to be reset at switching times to ensure both continuity and smoothness of the control signal $u(k)$ [2].

Theorem 3.3.1. *Suppose that each of the candidate controllers have slow-fast decomposition (3.37), (3.38) satisfying Assumption 1 and suppose that at time k^* the online controller is switched from controller K_i to controller K_j. At k^*, let the states of the slow and fast controllers be reset as follows*

$$x_{cft}(k^*) = 0 \tag{3.42}$$

$$x_{cs}(k^*) = C_{cs}^{j+}[u(k^*-1) - (D_{cs}^j + D_{cf}^j e(k^*-1))] + \zeta \tag{3.43}$$

where C_{cs}^{j+} is the pseudoinverse matrix of C_{cs}^j and ζ is any element of the null space of C_{cs}^j;

$$C_{cs}^j \zeta = 0 \tag{3.44}$$

Then, bumpless transfer is achieved at the switching time k^* [2].

The goal of bumpless transfer is to avoid both discontinuity and fast transients induced by switching. In this strategy, it is achieved by initializing the state of the slow part of the new controller $K_{jslow}(s)$ after each switch to a value computed to assure continuity, and setting the state of the fast part $K_{jfast}(s)$ to zero.

3.4 Bumpless Transfer Based on Predictive Control

Taking into account the bumpless transfer strategies from the previous sections, an one step predictive controller was design solving an optimal control problem in order to choose the best control and output signals that were obtained by applying each one of the strategies. This is one of the main results of this work.

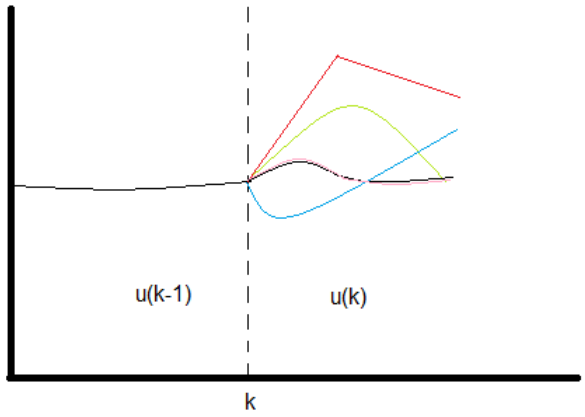

Figure 3.6: Control Signal Evolution with Bumpless Transfer Based on Predictive Control

Suppose that the i-th controller is *online* at time $k-1$ and that at time k the i-th controller is *online*. This means that k is the switching time. This algorithm, through the predictive controller, seeks to predict the optimal control and output signals by evaluating the difference between these signals in the times k and $k-1$ for each bumpless transfer strategy and choosing the one that minimizes an objective function.

For example, in figure 3.6, the optimal control signal is in black and at the switching instant, this algorithm evaluates each control signal previously obtained and chooses the one that exhibits a less bumpy behavior (in this case, the pink one).

3.4.1 Predictive Controller

To finally achieve bumpless transfer, optimal control signals are found minimizing equation (3.45) with respect to the control signal $\tilde{u}$ at the switching instants.

$$\Delta\tilde{u}' S \Delta\tilde{u} + \Delta y' R \Delta y \tag{3.45}$$

Where

$$\Delta\tilde{u} = u(k) - u(k-1) \tag{3.46}$$
$$\Delta y = y(k) - y(k-1) \tag{3.47}$$

And S, R are constant positive definite weighting matrices of the appropriate dimensions that can be modified to change the contribution of the online controller control signals and the plant outputs in the one step ahead prediction.

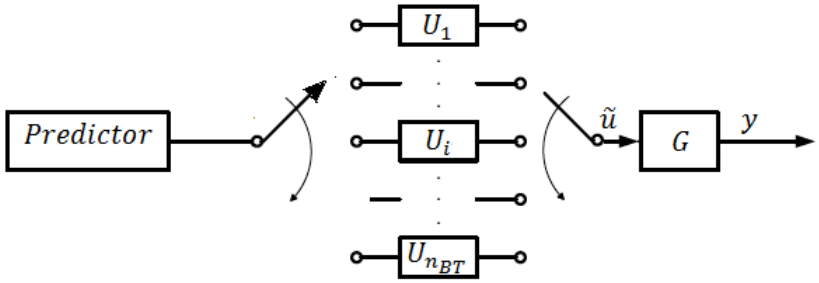

Figure 3.7: Bumpless Transfer Based on Predictive Control Scheme

At the switching instants, the optimal control signals take the value of the control signals found with the bumpless transfer methods previously discussed that minimize equation (3.45). And in the other times, the optimal control signals take the value of the control signals found switching the systems.

Suppose that, as mentioned before, the switching instant is k. Therefore,

$$u(k) \in \{U_1, U_2, U_3\} \tag{3.48}$$

where U_1 is the control space of the linear quadratic bumpless strategy, U_2 is the control space of the steady-state bumpless transfer under controller uncertainty using the state/output feedback topology strategy and U_3 is the control space of the bumpless transfer for adaptative switching controls strategy.

The optimal control signals at the switching instant are found evaluating the set of control and output signals in U_i, $i \in \{1, 2, 3\}$ in (3.45) choosing the control signals that minimize (3.45). This is shown in Fig. 3.7.

Chapter 4

Stability

Bumpless transfer techniques may lead to stability problems. If it is assumed that the online and offline controllers are stabilizing for the plant, around a certain operating point, the stability of the closed-loop system around this operating point, without switching occurring, is guaranteed. However, nothing can be concluded in general about the stability of the overall system when arbitrary switching occurs [1].

If the overall system is unstable for a determined bumpless transfer strategy, it is possible that the control signal do not behave as desired and the actuators saturate. The idea is to find a bumpless transfer strategy that guaranties the overall system's stability and that minimizes the discontinuities and bumps on the control signal.

Multiple Lyapunov functions are used to find the conditions such that the switched system is stable under any switching law s, using the closed loop system matrix and evaluating some linear matrices inequalities for all the switching cases available.

In this chapter, two theorems about stability for two bumpless transfer strategies and their respective demonstration are presented.

Assuming n_k controllers, if the i-th is the *online* controller and is desirable to switch to the j-th controller, the following conditions must be satisfied

$$\mathbb{A}_i' P_j \mathbb{A}_i - P_i < 0 \forall (i,j) \in QxQ \tag{4.1}$$

$$P_i > 0 \tag{4.2}$$

where $\mathbb{A}_i$ corresponds to the closed loop system matrix when the i-th controller is *online* and P_i, P_j are positive-definite matrices which are found solving the *LMI* with Sedumi-Yalmip. This is the theorem that guarantees GUES with multiple Lyapunov functions for discrete time.

4.1 Stability with Linear Quadratic Bumpless Transfer

Applying the linear quadratic bumpless transfer strategy on a system, stability for the overall system can be guaranteed if there exists a matrix F given by

$$F = (I - \Delta B_c^{2'} \Pi B_c^2)^{-1} \Delta \begin{bmatrix} (D_c^{2\prime} W_u C_c^2 + B_c^{2\prime} \Pi A_c^2)' \\ -(D_c^{2\prime} W_u + B_c^{2\prime} (I - M)^{-1} \hat{U})' \\ -(W_e + B_c^{2\prime} (I - M)^{-1} \hat{E})' \end{bmatrix} \tag{4.3}$$

And that satisfies theorem (4.1.1)

Theorem 4.1.1. ***(Stability LQBT)*** *Suppose a system with n_k controllers, and assume that the i-th controller is online. If the linear quadratic bumpless transfer strategy is applied, the system is stable if there exists a matrix F such that equation (4.1) is satisfied $\forall (i,j) \in Q \times Q$, where*

$$\mathbb{A}_i = \begin{bmatrix} A^i + B^i D_c^i C^i & \cdots & 0 & B^i C_c^i & 0 & \cdots & 0 \\ \vdots & \ddots & \vdots & \vdots & \vdots & \vdots & \vdots \\ B_c^{i-1}(F_u^{i-1} D_c^i F_e^{i-1}) C^i & \cdots & A_c^{i-1} + B_c^{i-1} F_x^{i-1} & B_c^{i-1} F_u^{i-1} C_c^i & 0 & \cdots & 0 \\ B_c^i C^i & \cdots & 0 & A_c^i & 0 & \cdots & 0 \\ B_c^{i+1}(F_u^{i+1} D_c^i - F_e^{i+1}) C^i & \cdots & 0 & B_c^{i+1} F_u^{i+1} C_c^i & A_c^{i+1} + B_c^{i+1} F_x^{i+1} & \cdots & 0 \\ \vdots & \vdots & \vdots & \vdots & \vdots & \vdots & \vdots \\ B_c^{n_k}(F_u^{n_k} D_c^i - F_e^{n_k}) C^i & \cdots & 0 & B_c^{n_k} F_u^{n_k} C_c^i & 0 & \cdots & A_c^{n_k} + B_c^{n_k} F_x^{n_k} \end{bmatrix} \tag{4.4}$$

Where A^i, B^i, C^i, D^i are the state space equations of the plant G_i, (taken as A, B, C, D for $i = 1$). A_c^i, B_c^i, C_c^i, D_c^i are the state space equations of the controller K_i, (taken as A_c, B_c, C_c, D_c for $i = 1$). And F_x^j, F_u^j, F_x^j are the components of the matrix F found when the j-th controller is offline (taken as F_x, F_u, F_e for $i = 1$).

And, the matrix $\mathbb{A}_i$ has dimensions $n+n_cn_k, n+n_cn_k$ where n is the number of states of the plant, n_c is the number of states of the controller and n_k is the number of controllers.

Proof. Assuming that there are two controllers for the system, we proceed to find the closed loop system matrix.

Assuming that the controller 1 is *online*, we have

$$x(k+1) = Ax(k) + B\tilde{u}(k) \tag{4.5}$$
$$y(k) = Cx(k) \tag{4.6}$$

$$x_c(k+1) = A_cx_c(k) + B_cy(k) \tag{4.7}$$
$$\tilde{u}(k) = C_cx_c(k) + D_cy(k) \tag{4.8}$$

Then

$$x(k+1) = Ax(k) + B(C_cx_c(k) + D_cy(k)) \tag{4.9}$$
$$= Ax(k) + B(C_cx_c(k) + D_cCx(k)) \tag{4.10}$$
$$= Ax(k) + BC_cx_c(k) + BD_cCx(k) \tag{4.11}$$
$$= (A + BD_cC)x(k) + BC_cx_c(k) \tag{4.12}$$
$$x_c(k+1) = B_cCx(k) + A_cx_c(k) \tag{4.13}$$
$$\begin{bmatrix} x(k+1) \\ x_c(k+1) \end{bmatrix} = \begin{bmatrix} A + BD_cC & BC_c \\ B_cC & A_c \end{bmatrix} \begin{bmatrix} x(k) \\ x_c(k) \end{bmatrix} \tag{4.14}$$

For the *offline* controller (2), we have

$$x_c^2(k+1) = A_c^2x_c^2(k) + B_c^2\alpha(k) \tag{4.15}$$
$$u(k) = C_c^2x_c^2(k) + D_c^2\alpha(k) \tag{4.16}$$

$$\begin{aligned}\alpha(k) =& F\begin{bmatrix}x_c^2(k) & \tilde{u}(k) & e(k)\end{bmatrix} && (4.17)\\ =& F_x^2 x_c^2(k) + F_u^2\tilde{u}(k) + F_e^2 e(k) && (4.18)\end{aligned}$$

with

$$\begin{aligned}F_u\tilde{u}(k) =& F_u^2(C_c x_c(k) + D_c y(k)) && (4.19)\\ =& F_u^2(C_c x_c(k) + D_c C x(k)) && (4.20)\\ =& F_u^2 D_c C x(k) + F_u^2 C_c x_c(k) && (4.21)\\ F_e^2 e(k) =& - F_e^2 C x(k) && (4.22)\end{aligned}$$

Then

$$\begin{aligned}\alpha(k) =& F_x^2 x_c^2(k) + F_u^2 D_c C x(k) + F_u^2 C_c x_c(k) - F_e^2 C x(k) && (4.23)\\ =& (F_u^2 D_c C - F_e^2 C)x(k) + F_u^2 C_c x_c(k) + F_x^2 x_c^2(k) && (4.24)\end{aligned}$$

and

$$\begin{aligned}x_c^2(k+1) =& A_c^2 x_c^2(k) + B_c^2((F_u^2 D_c C - F_e^2 C)x(k) + F_u^2 C_c x_c(k) + F_x^2 x_c^2(k)) && (4.25)\\ =& A_c^2 x_c^2(k) + (B_c^2 F_u^2 D_c C - B_c^2 F_e^2 C)x(k) + B_c^2 F_u^2 C_c x_c(k) + B_c^2 F_x^2 x_c^2(k)) && (4.26)\\ =& (B_c^2 F_u^2 D_c C - B_c^2 F_e^2 C)x(k) + B_c^2 F_u^2 C_c x_c(k) + (A_c^2 + B_c^2 F_x^2)x_c^2(k) && (4.27)\end{aligned}$$

$$\begin{bmatrix}x(k+1)\\ x_c(k+1)\\ x_c^2(k+1)\end{bmatrix} = \begin{bmatrix}A + BD_cC & BC_c & 0\\ B_cC & A_c & 0\\ B_c^2F_u^2D_cC - B_c^2F_e^2C & B_c^2F_u^2C_c & A_c^2 + B_c^2F_x^2\end{bmatrix}\begin{bmatrix}x(k)\\ x_c(k)\\ x_c^2(k)\end{bmatrix} \quad (4.28)$$

To derive the equation for the general case, with n controllers, we assume that the i-th controller is online and we obtain

$$\mathbb{A}_i = \begin{bmatrix} A^i + B^i D_c^i C^i & \cdots & 0 & B^i C_c^i & 0 & \cdots & 0\\ \vdots & \ddots & \vdots & \vdots & \vdots & \vdots & \vdots\\ B_c^{i-1}(F_u^{i-1}D_c^i F_e^{i-1})C^i & \cdots & A_c^{i-1} + B_c^{i-1}F_x^{i-1} & B_c^{i-1}F_u^{i-1}C_c^i & 0 & \cdots & 0\\ B_c^i C^i & \cdots & 0 & A_c^i & 0 & \cdots & 0\\ B_c^{i+1}(F_u^{i+1}D_c^i - F_e^{i+1})C^i & \cdots & 0 & B_c^{i+1}F_u^{i+1}C_c^i & A_c^{i+1} + B_c^{i+1}F_x^{i+1} & \cdots & 0\\ \vdots & \vdots & \vdots & \vdots & \vdots & \vdots & \vdots\\ B_c^{n_k}(F_u^{n_k}D_c^i - F_e^{n_k})C^i & \cdots & 0 & B_c^{n_k}F_u^{n_k}C_c^i & 0 & \cdots & A_c^{n_k} + B_c^{n_k}F_x^{n_k}\end{bmatrix} \quad (4.29)$$

□

This theorem gives the necessary conditions to choose the weighting matrices W_u and W_e of the difference between the control signals and the signals driving the controllers, respectively; in order to stabilize the overall system.

4.2 Stability with Steady-State Bumpless Transfer Under Controller Uncertainty Using the State/Output Feedback Topology

Applying the steady-state bumpless transfer under controller uncertainty using the state-output feedback topology strategy on a system, stability for the overall system can be guaranteed if there exists a matrix F given by

$$F = (I - \Delta B_c^{2'} \Pi B_c^2)^{-1} \Delta \begin{bmatrix} (D_c^{2\prime} W_u C_c^2 + B_c^{2\prime} \Pi A_c^2)' \\ -(D_c^{2\prime} W_u + B_c^{2\prime} (I - M)^{-1} \hat{U})' \\ -(W_e + B_c^{2\prime} (I - M)^{-1} \hat{E})' \end{bmatrix} \tag{4.30}$$

And a mismatch compensator K_{MC} with integral constants k_{int} that satisfies theorem (4.2.1)

Theorem 4.2.1. ***(Stability MC)*** *Suppose a system with 2 controllers, and assume that the first controller is online. If the steady-state bumpless transfer under controller uncertainty using the state/output feedback topology strategy is applied, the system is stable if there exists a matrix F and there are constants k_{int} such that matrices $\hat{\mathbb{A}}_1$, $\hat{\mathbb{A}}_2$ satisfy equation (4.1). Where,*

$$\hat{\mathbb{A}}_1 = \begin{bmatrix} A + BD_cC & BC_c & 0 & 0 & 0 \\ B_cC & A_c & 0 & 0 & 0 \\ -B_c^2(F_e^2 + F_u^2 \delta X^2 (D_c + \Delta_1^2))C & B_c^2 F_u^2 \delta X^2 C_c & A_c^2 + B_c^2 F_x^2 + B_c^2 F_u^2 \delta \Delta_2^2 & B_c^2 F_u^2 (I + \delta \Delta_3^2) & B_c^2 F_u^2 (I + \delta \Delta_4^2) \\ \Delta_1 & X^2 C_c & \Delta_2^2 & \Delta_3^2 & \Delta_4^2 \\ \delta \Delta_1^2 & \delta X^2 C_c & \delta \Delta_2^2 & I + \delta \Delta_3^2 & I + \delta \Delta_4^2 \end{bmatrix} \tag{4.31}$$

$$\hat{\mathbb{A}}_2 = \begin{bmatrix} A^2 + B^2 D_c^2 C^2 & 0 & B^2 C_c^2 & 0 & 0 \\ -B_c(F_e + F_u \delta X^1 (D_c + \Delta_1^1))C^2 & A_c + B_c F_x + B_c F_u \delta \Delta_2^1 & B_c F_u \delta X^1 C_c^2 & B_c F_u (I + \delta \Delta_3^1) & B_c F_u (I + \delta \Delta_4^1) \\ B_c^2 C^2 & 0 & A_c^2 & 0 & 0 \\ \Delta_1^1 & \Delta_2^1 & X^1 C_c^2 & \Delta_3^1 & \Delta_4^1 \\ \delta \Delta_1^1 & \delta \Delta_2 & \delta X^1 C_c^2 & I + \delta \Delta_3^1 & I + \delta \Delta_4^1 \end{bmatrix} \tag{4.32}$$

With

$$\delta = \frac{T_s}{2} k_{int} \tag{4.33}$$
$$X^i = (I + D_c^i F_u^i \delta)^{-1} \tag{4.34}$$
$$\Delta_1^i = X D_c^i F_e^i \tag{4.35}$$
$$\Delta_2^i = -X(C_c^i + D_c^i F_x^i) \tag{4.36}$$
$$\Delta 3^i = -X\delta D_c^i F_u^i \tag{4.37}$$
$$\Delta 4^i = -X k_{int} D_c^i F_u^i \tag{4.38}$$

Where A^i, B^i, C^i, D^i are the state space equations of the plant G_i, (taken as A, B, C, D for $i = 1$). A_c^i, B_c^i, C_c^i, D_c^i are the state space equations of the controller K_i, (taken as A_c, B_c, C_c, D_c for $i = 1$). And F_x^j, F_u^j, F_x^j are the components of the matrix F found when the j-th controller is offline (taken as F_x, F_u, F_e for $i = 1$).

Proof. Assuming that there are two controllers for the system, we proceed to find the closed loop system matrix.

Assuming that the controller 1 is *online*, we have

$$x(k+1) = Ax(k) + B\tilde{u}(k) \tag{4.39}$$
$$y(k) = Cx(k) \tag{4.40}$$

$$x_c(k+1) = A_c x_c(k) + B_c y(k) \tag{4.41}$$
$$\tilde{u}(k) = C_c x_c(k) + D_c y(k) \tag{4.42}$$

Then

$$\begin{bmatrix} x(k+1) \\ x_c(k+1) \end{bmatrix} = \begin{bmatrix} A + BD_cC & BC_c \\ B_cC & A_c \end{bmatrix} \begin{bmatrix} x(k) \\ x_c(k) \end{bmatrix} \tag{4.43}$$

For the *offline* controller (2), we have

$$x_c^2(k+1) = A_c^2 x_c^2(k) + B_c^2 \alpha(k) \tag{4.44}$$
$$u(k) = C_c^2 x_c^2(k) + D_c^2 \alpha(k) \tag{4.45}$$

$$\alpha(k) = F\begin{bmatrix} x_c^2(k) & e_0(k) & e(k) \end{bmatrix} \tag{4.46}$$
$$= F_x^2 x_c^2(k) + F_u^2 e_0(k) + F_e^2 e(k) \tag{4.47}$$

with

$$F_e^2 e(k) = -F_e^2 C x(k) \tag{4.48}$$
$$\tag{4.49}$$

Then

$$x_c^2(k+1) = A_c^2 x_c^2(k) + B_c^2(F_x^2 x_c^2(k) + F_u^2 e_0(k) - F_e^2 C x(k)) \tag{4.50}$$
$$= A_c^2 x_c^2(k) + B_c^2 F_x^2 x_c^2(k) + B_c^2 F_u^2 e_0(k) - B_c^2 F_e^2 C x(k) \tag{4.51}$$
$$= -B_c^2 F_e^2 C x(k) + (A_c^2 + B_c^2 F_x^2) x_c^2(k) + B_c^2 F_u^2 e_0(k) \tag{4.52}$$

Where $e_0(k)$ is the output signal of the mismatch compensator and is given by

$$e_0(k) = k_{int}[e_0(k-1) + \frac{T_s}{2}(\tilde{u}(k) - u(k) + \tilde{u}(k-1) - u(k-1))] \tag{4.53}$$

k_{int} is the vector integral constant and T_s is the sampling time. Taking $e_1(k) = e_0(k-1)$ and $u_0(k) = \tilde{u}(k-1) - u(k-1)$, we have

$$e_1(k+1) = e_0(k) \tag{4.54}$$
$$= k_{int}\left[e_1(k) + \frac{T_s}{2}(u_0(k) + u_0(k+1))\right] \tag{4.55}$$
$$u_0(k+1) = \tilde{u}(k) - u(k) \tag{4.56}$$
$$\tag{4.57}$$

Combining the previous equations, we have

$$u_0(k+1) = \tilde{u}(k) - u(k) \tag{4.58}$$
$$= C_c x_c(k) + D_c C x(k) - C_c^2 x_c^2(k) - D_c^2 \alpha(k) \tag{4.59}$$
$$= C_c x_c(k) + D_c C x(k) - C_c^2 x_c^2(k) - D_c^2 F_x^2 x_c^2(k) - D_c^2 F_u^2 e_0(k) + D_c^2 F_e^2 C x(k) \tag{4.60}$$
$$= (D_c + D_c^2 F_e^2) C x(k) + C_c x_c(k) - (C_c^2 + D_c^2 F_x^2) x_c^2(k) - D_c^2 F_u^2 e_0(k) \tag{4.61}$$

Taking $\delta = k_{int}\frac{T_s}{2}$,

$$e_0(k) = k_{int} e_1(k) + \delta u_0(k) + \delta u_0(k+1) \tag{4.62}$$

And

$$u_0(k+1) =(D_c + D_c^2F_e^2)Cx(k) + C_cx_c(k) - (C_c^2 + D_c^2F_x^2)x_c^2(k)- \tag{4.63}$$
$$D_c^2F_u^2(k_{int}e_1(k) + \delta u_0(k) + \delta u_0(k+1)) \tag{4.64}$$
$$(I + D_c^2F_u^2\delta)u_0(k+1) =(D_c + D_c^2F_e^2)Cx(k) + C_cx_c(k)- \tag{4.65}$$
$$(C_c^2 + D_c^2F_x^2)x_c^2(k) - D_c^2F_u^2(k_{int}e_1(k) + \delta u_0(k)) \tag{4.66}$$
$$u_0(k+1) =(I + D_c^2F_u^2\delta)^{-1}[(D_c + D_c^2F_e^2)Cx(k) + C_cx_c(k)- \tag{4.67}$$
$$(C_c^2 + D_c^2F_x^2)x_c^2(k) - D_c^2F_u^2(k_{int}e_1(k) + \delta u_0(k))] \tag{4.68}$$

Taking $X = (I + D_c^2F_u\delta)^{-1}$

$$u_0(k+1) = X[(D_c + D_c^2F_e^2)Cx(k) + C_cx_c(k) - (C_c^2 + D_c^2F_x^2)x_c^2(k) - D_c^2F_u^2(\delta u_0(k) + k_{int}e_1(k))] \tag{4.69}$$

Then

$$e_0(k) =k_{int}e_1(k) + \delta u_0(k) + \delta X[(D_c + D_c^2F_e^2)Cx(k) + C_cx_c(k)- \tag{4.70}$$
$$(C_c^2 + D_c^2F_x^2)x_c^2(k) - D_c^2F_u^2(\delta u_0(k) + k_{int}e_1(k))] \tag{4.71}$$
$$=\delta X[(D_c + D_c^2F_e^2)Cx(k) + C_cx_c(k) - (C_c^2 + D_c^2F_x^2)x_c^2(k)] \tag{4.72}$$
$$+ (1 - \delta XD_c^2F_u^2)(k_{int}e_1(k) + \delta u_0(k)) \tag{4.73}$$

And,

$$x_c^2(k+1) =- B_c^2F_e^2Cx(k) + (A_c^2 + B_c^2F_x^2)x_c^2(k) + \delta B_c^2F_u^2X[(D_c + D_c^2F_e)Cx(k) \tag{4.74}$$
$$+ C_cx_c(k) - (C_c^2 + D_c^2F_x^2)x_c^2(k)] + (1 - \delta XD_c^2F_u^2)(k_{int}e_1(k) + \delta u_0(k)) \tag{4.75}$$
$$=(-B_c^2F_e^2 + \delta B_c^2F_u^2(D_c + D_c^2F_e^2))Cx(k) + \delta B_c^2F_u^2C_cx_c(k)+ \tag{4.76}$$
$$(A_c^2 + B_c^2F_x^2 - \delta B_c^2F_u^2X(C_c^2 + D_c^2F_x^2))x_c^2(k) \tag{4.77}$$
$$+ B_c^2F_u^2(1 - \delta XD_c^2F_u^2)(k_{int}e_1(k) + \delta u_0(k)) \tag{4.78}$$

The state space equations are

$$x(k+1) =(A + BD_cC)x(k) + BC_cx_c(k) \tag{4.79}$$
$$xc(k+1) =B_cCx(k) + A_cx_c(k) \tag{4.80}$$
$$x_c^2(k+1) =(-B_c^2F_e^2 + \delta B_c^2F_u^2(D_c + D_c^2F_e^2)Cx(k) + \delta B_c^2F_u^2C_cx_c(k)+ \tag{4.81}$$
$$(A_c^2 + B_c^2F_x^2 - \delta B_c^2F_u^2X(C_c^2 + D_c^2F_x^2))x_c^2(k) \tag{4.82}$$
$$+ B_c^2F_u^2(1 - \delta XD_c^2F_u^2)(k_{int}e_1(k) + \delta u_0(k)) \tag{4.83}$$
$$u_0(k+1) =X[(D_c + D_c^2F_e^2)Cx(k) + C_cx_c(k) - (C_c^2 + D_c^2F_x^2)x_c^2(k) \tag{4.84}$$
$$- D_c^2F_u^2(\delta u_0(k) + k_{int}e_1(k))] \tag{4.85}$$
$$e_1(k+1) =\delta X[(D_c + D_c^2F_e^2)Cx(k) + C_cx_c(k) - (C_c^2 + D_c^2F_x^2)x_c^2(k)] \tag{4.86}$$
$$+ (1 - \delta XD_c^2F_u^2)(k_{int}e_1(k) + \delta u_0(k)) \tag{4.87}$$

$$\Delta_1^i = X D_c^i F_e^i \tag{4.88}$$
$$\Delta_2^i = -X(C_c^i + D_c^i F_x^i) \tag{4.89}$$
$$\Delta 3^i = -X\delta D_c^i F_u^i \tag{4.90}$$
$$\Delta 4^i = -X k_{int} D_c^i F_u^i \tag{4.91}$$

We have

$$\hat{\mathbb{A}}_1 = \begin{bmatrix} A + BD_cC & BC_c & 0 & 0 & 0 \\ B_cC & A_c & 0 & 0 & 0 \\ -B_c^2(F_e^2 + F_u^2\delta X^2(D_c + \Delta_1^2))C & B_c^2F_u^2\delta X^2C_c & A_c^2 + B_c^2F_x^2 + B_c^2F_u^2\delta\Delta_2^2 & B_c^2F_u^2(I + \delta\Delta_3^2) & B_c^2F_u^2(I + \delta\Delta_4^2) \\ \Delta_1 & X^2C_c & \Delta_2^2 & \Delta_3^2 & \Delta_4^2 \\ \delta\Delta_1^2 & \delta X^2C_c & \delta\Delta_2^2 & I + \delta\Delta_3^2 & I + \delta\Delta_4^2 \end{bmatrix} \tag{4.92}$$

$$\hat{\mathbb{A}}_2 = \begin{bmatrix} A^2 + B^2D_c^2C^2 & 0 & B^2C_c^2 & 0 & 0 \\ -B_c(F_e + F_u\delta X^1(D_c + \Delta_1^1))C^2 & A_c + B_cF_x + B_cF_u\delta\Delta_2^1 & B_cF_u\delta X^1C_c^2 & B_cF_u(I + \delta\Delta_3^1) & B_cF_u(I + \delta\Delta_4^1) \\ B_c^2C^2 & 0 & A_c^2 & 0 & 0 \\ \Delta_1^1 & \Delta_2^1 & X^1C_c^2 & \Delta_3^1 & \Delta_4^1 \\ \delta\Delta_1^1 & \delta\Delta_2 & \delta X^1C_c^2 & I + \delta\Delta_3^1 & I + \delta\Delta_4^1 \end{bmatrix} \tag{4.93}$$

□

This theorem gives the necessary conditions to choose the weighting matrices W_u and W_e of the difference between the control signals and the signals driving the controllers, respectively; and the integral constants of the mismatch compensator K_{MC} in order to stabilize the overall system.

With respect to the constant integrals, a stability interval can be found for each k_{int_i}, $i \in \{1, 2, ...p\}$.

Chapter 5

Results

The bumpless transfer strategies and stability theorems were applied on the web winding system of the control laboratory. In this chapter are presented the results obtained by applying each one of the bumpless transfer strategies and the comparison between them. Also, some analysis are given for each one.

In addition, the stability theorems found in the previous section are used and an example of an unstable case with the mismatch compensator is given. Finally, it is presented a comparison on the performance of the bumpless transfer algorithm obtained and the LPV control technique used on the web winding system of the control laboratory.

5.1 Simulation

The web winding system of the control laboratory has three models given by [9]:

$$x(k) = A^i x(k) + B^i \tilde{u}(k) \tag{5.1}$$

$$y(k) = C^i x(k) + D^i \tilde{u}(k) \tag{5.2}$$

- $i = 1$

$$A^1 = \begin{bmatrix} 0.97083 & -0.059253 & -0.00061709 & 0.11824 \\ 0.080598 & 0.90838 & 0.015871 & 0.45606 \\ -0.012797 & 0.064948 & 0.99256 & -0.038484 \\ -0.095656 & 0.11558 & -0.068102 & -0.0027797 \end{bmatrix} \tag{5.3}$$

$$B^1 = \begin{bmatrix} -0.38033 & 0.098706 \\ -1.0017 & 0.25606 \\ 0.1321 & -0.077344 \\ 2.2645 & -0.51136 \end{bmatrix} \tag{5.4}$$

$$C^1 = \begin{bmatrix} 1 & 0 & 0 & 0 \\ 0 & 1 & 0 & 0 \\ 0 & 0 & 1 & 0 \\ 0 & 0 & 0 & 1 \end{bmatrix} \tag{5.5}$$

$$D^1 = \begin{bmatrix} 0 & 0 & 0 & 0 \\ 0 & 0 & 0 & 0 \end{bmatrix} \tag{5.6}$$

- $i = 2$

$$A^2 = \begin{bmatrix} 0.98359 & -0.07594 & 0.25068 & 0.03082 \\ 0.016798 & 0.95052 & -0.038408 & 0.025226 \\ -0.040198 & 0.017543 & -0.029979 & -0.03078 \\ -0.0061372 & -0.063698 & -0.40673 & 1.0008 \end{bmatrix} \tag{5.7}$$

$$B^2 = \begin{bmatrix} 0.09914 & -0.98783 \\ 0.0057923 & 0.10865 \\ -0.16257 & 3.7196 \\ -0.033691 & 1.4289 \end{bmatrix} \tag{5.8}$$

$$C^2 = \begin{bmatrix} 1 & 0 & 0 & 0 \\ 0 & 1 & 0 & 0 \\ 0 & 0 & 1 & 0 \\ 0 & 0 & 0 & 1 \end{bmatrix} \tag{5.9}$$

$$D^2 = \begin{bmatrix} 0 & 0 & 0 & 0 \\ 0 & 0 & 0 & 0 \end{bmatrix} \tag{5.10}$$

- $i = 3$

$$A^3 = \begin{bmatrix} 0.97391 & -0.11548 & -0.076609 & -0.17306 \\ 0.0039941 & 0.91826 & -0.017033 & -0.21528 \\ 0.041221 & -0.15677 & 0.83912 & -0.04879 \\ -0.020094 & -0.083877 & 0.077934 & 0.20791 \end{bmatrix} \tag{5.11}$$

$$B^3 = \begin{bmatrix} 6.9966 & -4.8607 \\ 7.8533 & -5.0766 \\ 2.8608 & -2.6272 \\ 27 & -16.717 \end{bmatrix} \tag{5.12}$$

$$C^3 = \begin{bmatrix} 1 & 0 & 0 & 0 \\ 0 & 1 & 0 & 0 \\ 0 & 0 & 1 & 0 \\ 0 & 0 & 0 & 1 \end{bmatrix} \tag{5.13}$$

$$D^3 = \begin{bmatrix} 0 & 0 & 0 & 0 \\ 0 & 0 & 0 & 0 \end{bmatrix} \tag{5.14}$$

Where the switching time is $T_s = 0.01s$

The procedure used to simulate this system with the bumpless transfer strategies was:

1. The disturbance matrices were added on each one of these models and the $\mathcal{H}_\infty$ controllers were design based on the results obtain from theorem 2.2.1 and solving the LMI with Sedumi-Yalmip.

2. The bumpless transfer strategies were implemented as shown in chapter 3 and with the characteristics presented in this chapter for each one. The system was simulated with initial condition $x(1) = [2\ 2\ 1\ 1]$ and a reference signal equal to zero.

3. The stability theorems were implemented and proven, and an unstable case was found for the mismatch compensator.

4. Different control laws were used to simulate the system and to observe the control signals and the system outputs. The control law used on the results figures is $s = [1\ 2\ 3]$, switching every 10 seconds.

5.2 $\mathcal{H}_\infty$ controller

The $\mathcal{H}_\infty$ controllers design for each one of the models, are given by:

$$x(k) = A_c^i x(k) + B_c^i y(k) \tag{5.15}$$
$$y(k) = C_c^i x(k) + D_c^i y(k) \tag{5.16}$$

- $i = 1$

$$A_c^1 = \begin{bmatrix} -0.0313 & -0.0049 & -0.0066 & 0.0124 \\ 0.0411 & -0.0617 & -0.1685 & 0.1794 \\ -0.0026 & -0.0053 & -0.0049 & 0.0072 \\ 0.0219 & -0.0167- & 0.0441 & 0.0400 \end{bmatrix} \tag{5.17}$$

$$B_c^1 = \begin{bmatrix} 1.3359 & -0.3539 & 0.1491 & 0.0191 \\ -0.2882 & 0.8784 & 0.4760 & 0.3176 \\ 0.1750 & 0.4649 & 0.3279 & 0.2159 \\ 0.0851 & 0.2990 & 0.2149 & 0.1319 \end{bmatrix} \tag{5.18}$$

$$C_c^1 = \begin{bmatrix} 0.1918 & -0.2650 & -0.7130 & 0.7290 \\ 0.8010 & -1.1664 & -3.1621 & 3.2701 \end{bmatrix} \tag{5.19}$$

$$D_c^1 = \begin{bmatrix} 1.1162 & -6.7048 & 1.0308 & -3.0086 \\ 3.0474 & -28.8969 & 4.2851 & -13.3017 \end{bmatrix} \tag{5.20}$$

- $i = 2$

$$A_c^2 = \begin{bmatrix} -0.1184 & -0.0236 & 0.0444 & -0.0578 \\ -0.1489 & -0.0601 & 0.0315 & -0.0850 \\ -0.0081 & -0.0088 & 0.0082 & -0.0158 \\ 0.0055 & 0.0060 & -0.0288 & 0.0198 \end{bmatrix} \tag{5.21}$$

$$B_c^2 = \begin{bmatrix} 0.3965 & -0.2462 & 0.3839 & -0.7058 \\ -0.2592 & 2.9018 & 0.0149 & -0.4502 \\ 0.3754 & 0.0817 & 0.3984 & -0.7804 \\ -0.6930 & -0.5773 & -0.7660 & 1.5682 \end{bmatrix} \tag{5.22}$$

$$C_2 = \begin{bmatrix} -3.9048 & -0.8538 & 0.9101 & -1.6770 \\ -0.1671 & -0.0393 & 0.0342 & -0.0733 \end{bmatrix} \tag{5.23}$$

$$D_c^2 = \begin{bmatrix} -14.2430 & -11.8258 & -2.0227 & -2.8223 \\ -0.5412 & -0.7117 & -0.0214 & -0.1982 \end{bmatrix} \tag{5.24}$$

- $i = 3$

$$A_c^3 = \begin{bmatrix} -0.0186 & 0.0205 & -0.0052 & 0.1572 \\ -0.1019 & -0.1370 & -0.1334 & -0.5780 \\ -0.0040 & 0.0024 & 0.0037 & 0.0279 \\ 0.0203 & 0.0230 & 0.0258 & 0.0807 \end{bmatrix} \tag{5.25}$$

$$B_{3=} \begin{bmatrix} 1.9260 & -3.2076 & -0.3946 & 0.4008 \\ -3.2126 & 9.6039 & -0.4332 & -1.6523 \\ -0.3801 & -0.4075 & 0.3461 & 0.1680 \\ 0.4666 & -1.9119 & 0.1891 & 0.3749 \end{bmatrix} \tag{5.26}$$

$$C_{3=} \begin{bmatrix} 0.0444 & 0.0207 & 0.0329 & 0.0092 \\ 0.0718 & 0.0333 & 0.0531 & 0.0168 \end{bmatrix} \tag{5.27}$$

$$D_{3=} \begin{bmatrix} 0.6771 & -0.2943 & 0.2335 & -0.1366 \\ 1.0688 & -0.3310 & 0.3600 & -0.2431 \end{bmatrix} \tag{5.28}$$

It is worth mentioning that the $\mathcal{H}_\infty$ controllers designed in these project have four states, six orders less than the controllers design in [9] for this system and are much faster.

5.3 Linear Quadratic Bumpless Transfer

The procedure shown in section 3.1 was applied to achieve linear quadratic bumpless transfer, varying the weighting matrices W_u and W_e in such a way that the Ricatti equation could be solved and that the closed loop system was stable (by looking at the eigenvalues of the closed loop system A matrix).

The following weighting matrices were used for each one of the subsystems, where the signals driving the controllers are given more importance than the control signals of these controllers (this is clear on the choose of the factor that precedes the identity matrices) .

$$W_u = 0.01 \begin{bmatrix} 1 & 0 \\ 0 & 1 \end{bmatrix} \tag{5.29}$$

$$W_e = 100 \begin{bmatrix} 1 & 0 & 0 & 0 \\ 0 & 1 & 0 & 0 \\ 0 & 0 & 1 & 0 \\ 0 & 0 & 0 & 1 \end{bmatrix} \tag{5.30}$$

Switching every 10 seconds, the following results were found for the previously described simulations, linear quadratic bumpless transfer strategy in blue and without applying it in red.

In the figure 5.5, it is shown that the linear quadratic bumpless transfer strategy minimizes the discontinuities on the control signals at the switching instants and the signals are much more softer when little bumps take place.

In the output signals can be observed a huge improvement by applying the linear quadratic bumpless transfer strategy.

For the first control signal, it can be appreciated that at the first switching instant $k = 10$, the transfer produces a bump (red) and the strategy reduces it in a considerable way (blue). For this reason, in the first output signal, the strategy produces a softer signal (blue) and the bump (red) disappears. At the second

switching instant $k = 20$, the strategy presents little reductions on the bumps form both, the first control and first output signals.

For the second control signal, it can be appreciated a softer behavior and the strategy reduces the bumps in a small percentage for both switchings. Therefore, the analog situation can be observed in the second output signal.

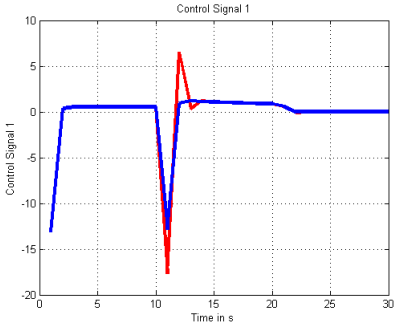

Figure 5.1: First Control Signal.

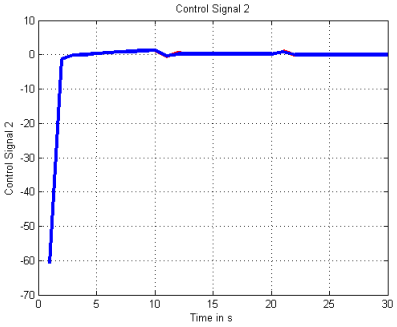

Figure 5.3: Second Control Signal.

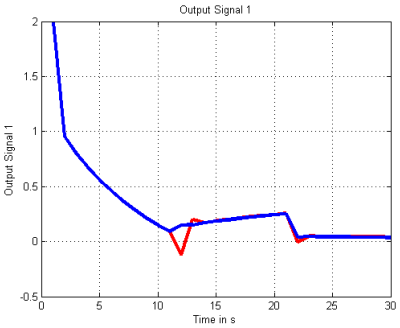

Figure 5.2: First System Output.

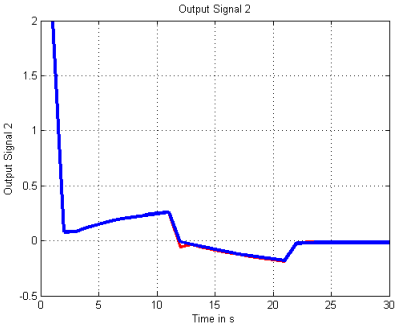

Figure 5.4: Second System Output.

Figure 5.5: Linear Quadratic Bumpless Transfer in Blue and Without in Red. Switching Law s=[1,2,3]

5.4 Steady-State Bumpless Transfer Under Controller Uncertainty Using the State/Output Feedback Topology

The procedure shown section 3.2 was applied to achieve bumpless transfer, using discrete integrators: An integrator has a transfer function given by

$$\frac{k_{int}}{s} \tag{5.31}$$

The discrete transfer function using 'Tustin' is

$$k_{int}\frac{\frac{T_s}{2}z + \frac{T_s}{2}}{z-1} \tag{5.32}$$

Where T_s is the sampling time (in this case, $T_s = 0.01$), and k_{int} is the integral constant. The associated difference equation is

$$y(k) = k_{int}\left(y(k-1) + \frac{T_s}{2}\left(u(k) + u(k-1)\right)\right) \tag{5.33}$$

which was implemented in Matlab. As there are two control signals, $k_{int} = \{k_{int_1}, k_{int_2}\}$

Switching every 10 seconds, the following results were found for the previously described simulations, applying the steady-state bumpless transfer under controller uncertainty using the state/output feedback topology strategy in black and without applying it in red. With $k_{int_1} = 0.4$ and $k_{int_2} = 0.2$.

In the figure 5.10, it is shown that the steady-state bumpless transfer under controller uncertainty using the state/output feedback topology strategy minimizes the discontinuities on the control signals at the switching instants and the signals are much more softer when little bumps take place.

In the output signals can be observed a huge improvement by applying the steady-state bumpless transfer under controller uncertainty using the state/output feedback topology strategy.

For the first control signal, it can be appreciated that at the first switching instant $k = 10$, the transfer produces a bump (red) and the strategy reduces it in a considerable way (blue). For this reason, in the first output signal, the strategy produces a softer signal (blue) and the bump (red) disappears. At the second switching instant $k = 20$, the strategy presents little reductions on the bumps form both, the first control and first output signals.

For the second control signal, it can be appreciated a softer behavior and the strategy reduces the bumps in a small percentage for both switchings. Therefore, the analog situation can be observed in the second output signal.

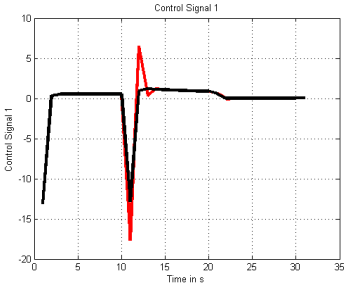

Figure 5.6: First Control Signal.

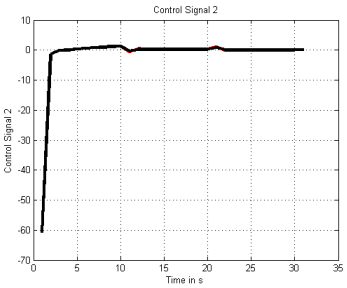

Figure 5.8: Second Control Signal.

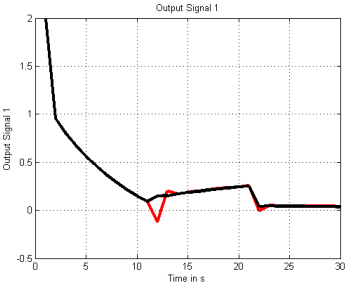

Figure 5.7: First System Output.

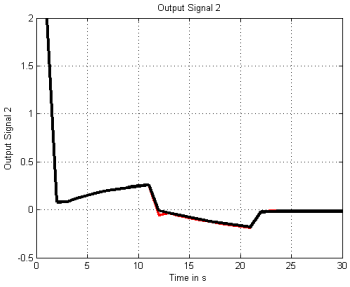

Figure 5.9: Second System Output.

Figure 5.10: Steady-State Bumpless Transfer Under Controller Uncertainty Using the State/Output Feedback Topology in Black and Without in Red. Switching Law s=[1,2,3]

5.5 Bumpless Transfer for Adaptive Switching Controls

The procedure shown in section 3.3 was applied to achieve bumpless transfer for adaptive switching controls, using the slowfast algorithm in Matlab [19] and reseting the slow and fast states of the controllers as shown in theorem 3.3.1.

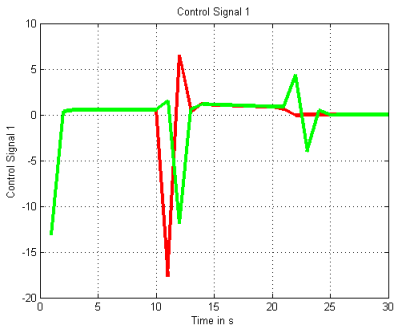

Figure 5.11: First Control Signal.

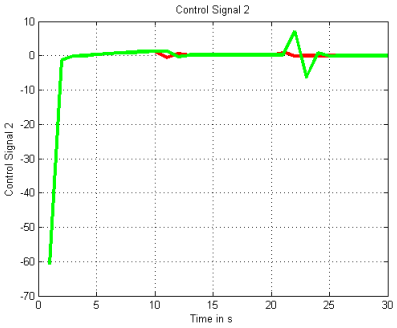

Figure 5.13: Second Control Signal.

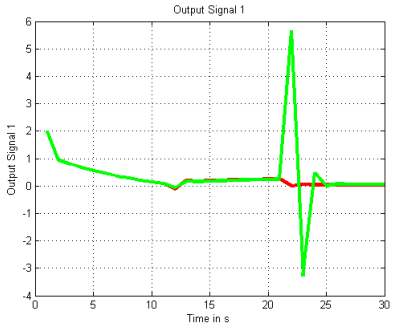

Figure 5.12: First System Output.

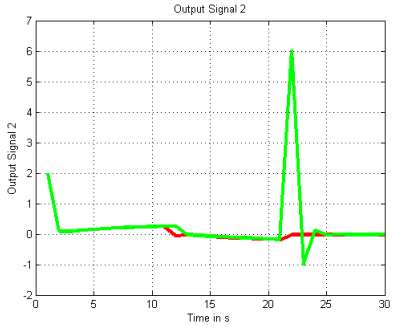

Figure 5.14: Second System Output.

Figure 5.15: Bumpless Transfer for Adaptive Switching Controls in Green and Without in Red. Switching Law s=[1,2,3]

Switching every 10 seconds, the following results were found for the previously described simulations, applying the bumpless transfer for adaptive switching controls strategy in green and without applying it in red.

In the figure 5.15, it is shown that the bumpless transfer for adaptive switching controls strategy minimizes the bumps at the first switching instant but does not minimize the discontinuities on the control signals at the second switching instant and instead, these signals present even bigger bumps. In the output signals the same behavior is evidenced.

For the first control signal, it can be appreciated that at the first switching instant $k = 10$, the transfer produces a bump (red) and the strategy reduces it in a considerable way (green). For this reason, in the first output signal, the strategy produces a softer signal (green) and the bump (red) disappears.

For the first control signals, it is observed that at the second switching instant $k = 20$, the strategy produces a bigger bump (green) that the one obtained when switching (red) and hence, the second output signal presents a bumpy behavior (green).

For the second control and output signal, an analog behavior is presented. At the first switching time $k = 10$, the bump (red) is reduced but at the second switching time $k = 20$, the strategy produces a bigger bump (green).

From the results, it can be concluded that this is not a reliable strategy because it produces undesired behaviors and due to the re-initialization of the states of the low and fast modes, it only assures (in some case) no bumps at the switching instant, which do not guarantee there will be no transient problems with infinite combinations of the controller states (no matter on the value of the control signal).

5.6 Bumpless Transfer Based on Predictive Control

The procedure shown in section 3.4 was applied to achieve bumpless transfer based on predictive control, where matrices S and R were chosen as

$$S = 0.3 \begin{bmatrix} 1 & 0 \\ 0 & 1 \end{bmatrix} \tag{5.34}$$

$$R = 0.7 \begin{bmatrix} 1 & 0 \\ 0 & 1 \end{bmatrix} \tag{5.35}$$

In this way, more importance was given to the output signals.

Switching every 10 seconds, the following results were found for the previously described simulations, applying the bumpless transfer based on predictive control strategy in yellow and without applying it in red.

In the figure 5.20, it is shown that the bumpless transfer based on predictive control strategy minimizes the discontinuities on the control and output signals at the switching instants and the signals are much more softer when little bumps take place.

For the first control signal, it can be appreciated that at the first switching instant $k = 10$, the transfer produces a bump (red) and the strategy reduces it in a considerable way (yellow). For this reason, in the first output signal, the strategy produces a softer signal (yellow) and the bump (red) disappears. At the second switching instant $k = 20$, the strategy presents little reductions on the bumps form both, the first control and first output signals.

For the second control signal, it can be appreciated a softer behavior and the strategy reduces the bumps in a small percentage for both switchings. Therefore, the analog situation can be observed in the second output signal.

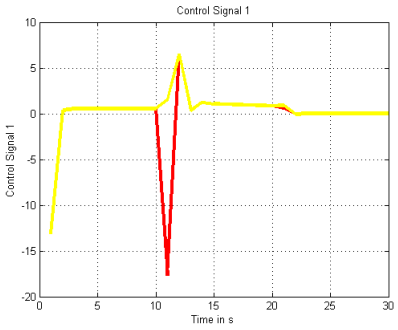

Figure 5.16: First Control Signal.

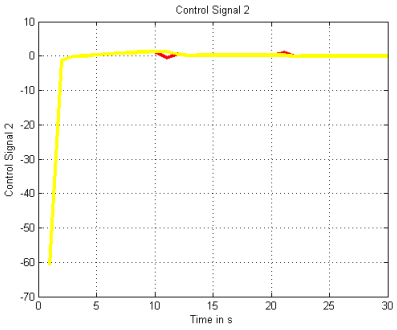

Figure 5.18: Second Control Signal.

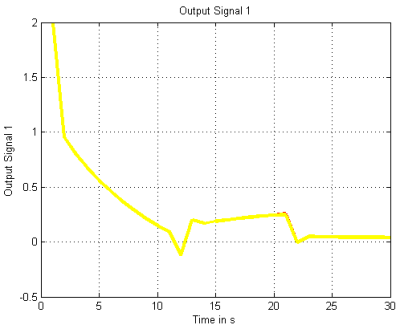

Figure 5.17: First System Output.

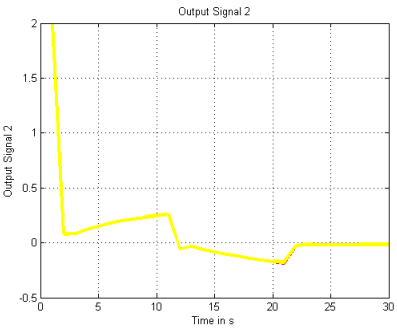

Figure 5.19: Second System Output.

Figure 5.20: Bumpless Transfer Based on Predictive Control in Yellow and Without in Red. Switching Law s=[1,2,3]

5.7 Comparison Between the Bumpless Transfer Strategies Used

Switching every 10 seconds, the following results were found for the previously described simulations, applying the linear quadratic bumpless transfer strategy in blue, the bumpless transfer for adaptive switching controls strategy in green, the steady-state bumpless transfer under controller uncertainty using the state/output feedback topology strategy in black, the bumpless transfer based on predictive control strategy in yellow and without applying them in red.

It can be appreciated that the linear quadratic bumpless strategy presented a very good behavior by minimizing the bumps in both, the control and output signals. However, these discontinuities could not be totally removed.

For the steady-state bumpless transfer under controller uncertainty using the state/output feedback topology strategy, the mismatch compensator did not improved the behavior reached by the linear quadratic bumpless strategy, but, the choice of the integrator constant values allowed to find the unstable case (as will be seen in the proceeding section).

The bumpless transfer for adaptive switching controls strategy presented the worst behavior because at the second switching instant increased the bumps in the control and output signals. And even though this strategy minimized the discontinuities in the signals at the first switching instants, the bumps were greater than the ones produced by the linear quadratic bumpless strategy.

The bumpless transfer based on predictive control strategy produced the best control signals by presenting the smallest bumps. Also, the output signals follow the ones found with the linear quadratic bumpless trasnfer strategy because these ones presented the best behavior.

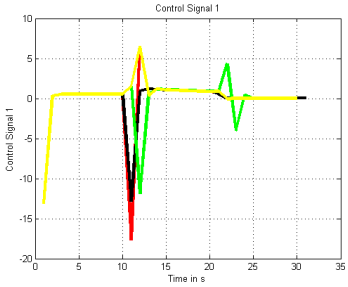

Figure 5.21: First Control Signal.

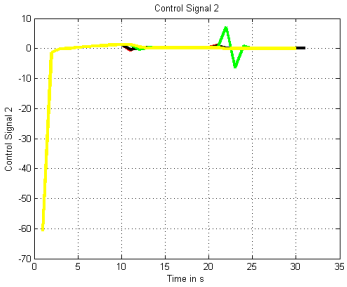

Figure 5.23: Second Control Signal.

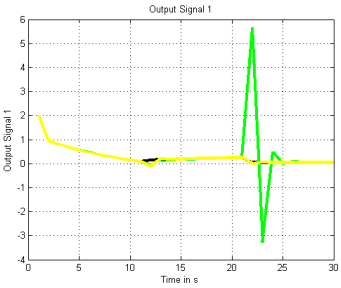

Figure 5.22: First System Output.

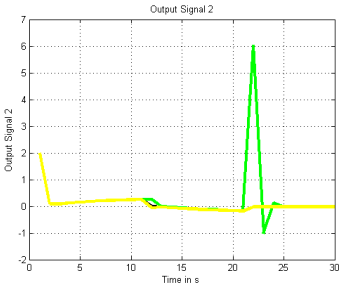

Figure 5.24: Second System Output.

Figure 5.25: Comparison among the Bumpless Transfer strategies used with Switching Law s=[1,2,3]. Linear Quadratic Bumpless Transfer in Blue, Steady-State Bumpless Transfer Under Controller Uncertainty Using the State/Output Feedback Topology Black, Bumpless Transfer for Adaptive Switching Controls in Green, Bumpless Transfer Based on Predictive Control in Yellow and Without in Red.

5.8 Stability

5.8.1 Stability with Linear Quadratic Bumpless Transfer

Varying the weighting matrices W_u and W_e the stability condition given by theorem (4.1.1) was verified and two cases were obtained.

- If $W_u << W_e$, The *LMI* that allows to find the matriz F is solved and the system is stable.
- IF $W_e << W_u$, it is not possible to solve the Ricatti equation that leads to the solution of the *LMI*.

5.8.2 Stability with Steady-State Bumpless Transfer Under Controller Uncertainty Using the State/Output Feedback Topology

When implementing the mismatch compensator, if the integral constants are greater than one, the stability condition given by equation theorem (4.2.1) is not verified and the system is unstable.

For example, for $k_{int} = 4$, the control and output signals are

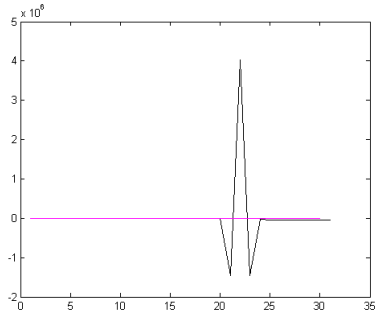

Figure 5.26: First Control Signal.

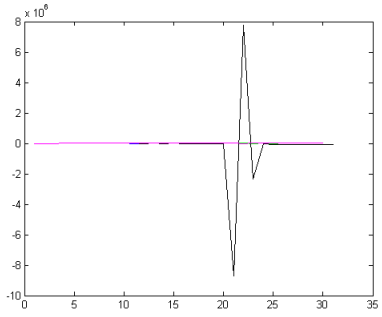

Figure 5.28: Second Control Signal.

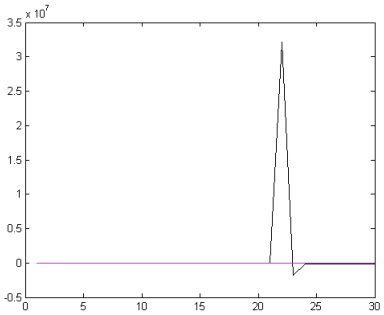

Figure 5.27: First System Output.

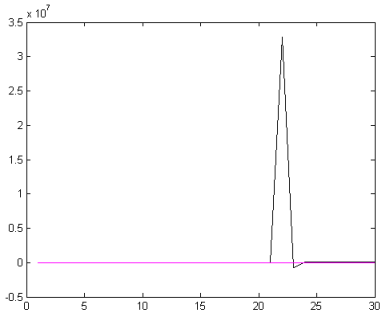

Figure 5.29: Second System Output.

Figure 5.30: Unstable Case $k_{int} = 4$ with Switching Law s=[1,2,3]

The unstable behavior can be observed in the control and output signals.

5.9 Comparison with the LPV Technique

Switching every 10 seconds, the following results were found for the LPV technique in blue.

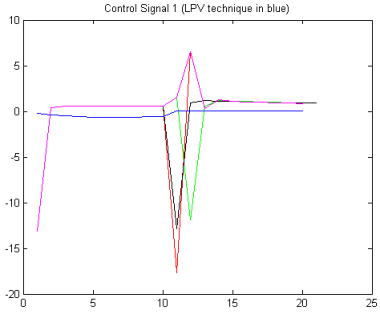

Figure 5.31: First Control Signal.

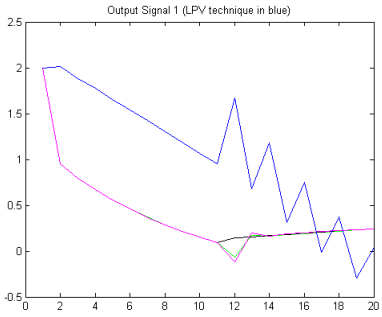

Figure 5.32: First System Output.

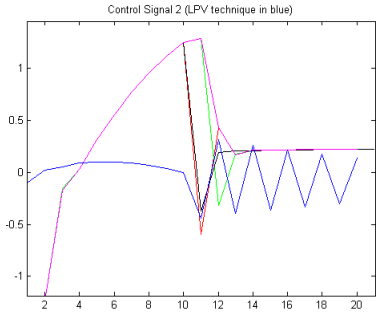

Figure 5.33: Second Control Signal.

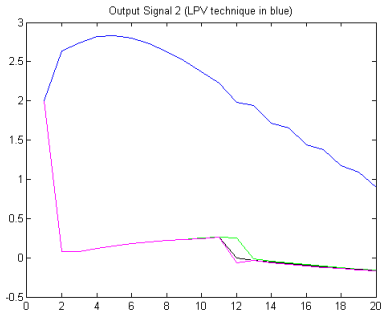

Figure 5.34: Second System Output.

Figure 5.35: Unstable Case $k_{int} = 4$ with Switching Law s=[1,2]

In the figure (5.35), it is shown that the LPV technique is not appropriated when switching systems. For the first control signal, Fig. (5.31), can be observed an offset but not bumps are present. In the second control signal, Fig. (5.33), a ripple appears after the switching time and this leads to an unstable behavior. As the control signals are no ideal, it is logical that the output signals do not present the desired behavior as is evidenced in Fig. (5.32) and Fig. (5.34).

For times greater or equal than 30, the four signals become unstable and if implemented in practice, with the LPV technique, the tape would probably break.

Chapter 6

Conclusions and Final Remarks

The linear quadratic bumpless transfer strategy [1] minimized the discontinuities and bumps in the control signals applied to the simulation on the web winding system of the control laboratory. For this reason, in the output signals could be observed a huge improvement by presenting little bumps when the switching instants took place.

The bumpless transfer for adaptive switching controls strategy did not work as hoped because at the switching instants, the control signals can present little or even bigger bumps and this behavior is not reliable in any application. That was evidenced in the output signals because the bumps increased significantly.

In the steady-state bumpless transfer under controller uncertainty using the state/output feedback topology strategy, the mismatch compensator exhibited the same behavior reached by the linear quadratic bumpless strategy. However, as the mismatch compensator is found to be a bank of integral controllers, the choice of the integrator constant values allowed to find the unstable case when they were greater than one through multiple Lyapunov functions and finding the closed loop system matrices.

The bumpless transfer based on predictive control strategy consisted on an optimal control problem used to find the best control/output signals for the web

winding system. These strategy presented the best results and can be implemented for bumpless transfer on switched systems.

For the linear quadratic bumpless transfer strategy, besides minimizing the discontinuities and bumps, stability was guaranteed on the overall system when arbitrary switching occurs through multiple Lyapunov functions. Therefore, this strategy is valid when dealing with switched systems.

The constants of the bank of integrators given by the mismatch compensator affect the stability of the overall system and when these constants are greater than one, the system is unstable. This shows that the bumpless transfer techniques lead to stability problems of the overall system when arbitrary switching occurs.

The LPV technique should not be implemented on switched systems with ambiguous switching laws because the system becomes unstable and in practice it would probably damage the plant.

Chapter 7

Appendix A

7.1 $\mathcal{H}_\infty$ Norms

Most of the analysis and synthesis will be done on a unified linear fractional transformation (LFT) framework as shown in figure 7.1. Where P is the interconnection matrix, K is the controller, Δ is the set of all possible uncertainty, w is a vector signal including noises, disturbances, and reference signals, z is a vector signal including all controlled signals and tracking errors, u is the control signal, and y is the measurement. [16]

The block diagram in figure 7.1 represents the following equations:

$$\begin{bmatrix} v \\ z \\ y \end{bmatrix} = P \begin{bmatrix} \eta \\ w \\ u \end{bmatrix} \tag{7.1}$$

$$\eta = \Delta v \tag{7.2}$$

$$u = Ky \tag{7.3}$$

Let the transfer matrix from w to z be denoted by T_{zw} and assume that the admissible uncertainty Δ satisfies $||\Delta||_\infty < 1/\gamma_u$ for some $\gamma_u > 0$. Then our analysis problem is to answer if the closed-loop system is stable for all admissible Δ and $||T_{zw}||_\infty \leq \gamma_p$ for some pre specified $\gamma_p > 0$, where $||T_{zw}||_\infty$ is the $\mathcal{H}_\infty$ norm defined

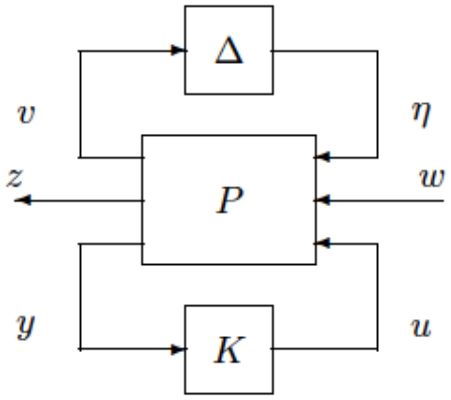

Figure 7.1: General LFT Framework. [16]

as $||T_{zw}||_\infty = \sup_w \bar{\sigma}(T_{zw}(jw))$. The synthesis problem is to design a controller K so that the afore mentioned robust stability and performance conditions are satisfied.

In the simplest form, we have either $\Delta = 0$ or $w = 0$. The former becomes the well-known $\mathcal{H}_\infty$ control problem and the later becomes the robust stability problem. The two problems are equivalent when Δ is a single-block unstructured uncertainty through the application of the small gain theorem. This robust stability consequence was probably the main motivation for the development of $\mathcal{H}_\infty$ methods. The analysis and synthesis for systems with multiple-block Δ can be reduced in most cases to an equivalent $\mathcal{H}_\infty$ problem with suitable scalings [16].

7.1.1 $\mathcal{H}_\infty$ Space

$\mathcal{L}_\infty$ $(j\mathbb{R})$ Space

$\mathcal{L}_\infty$ $(j\mathbb{R})$ or simply $\mathcal{L}_\infty$ is a Banach space of matrix valued (or scalar-valued) functions that are (essentially) bounded on $j\mathbb{R}$), with norm [16]

$$||F|||_\infty := ess \sup_{w \in \mathbb{R}} \bar{\sigma}[F(jw)] \tag{7.4}$$

The rational subspace of $\mathcal{L}_\infty$, denoted by $\mathcal{RL}_\infty(j\mathbb{R})$ or simply $\mathcal{RL}_\infty$, consists of all proper and real rational transfer matrices with no poles on the imaginary axis.

$\mathcal{H}_\infty$ Space

$\mathcal{H}_\infty$ is a (closed) subspace of $\mathcal{H}_\infty$ with functions that are analytic and bounded in the open right-half plane. The $\mathcal{H}_\infty$ norm is defined as [16]

$$||F|||_\infty := \sup_{Re(s)>0} \bar{\sigma}[F(s)] = \sup_{w\in\mathbb{R}} \bar{\sigma}[F(jw)] \tag{7.5}$$

The second equality can be regarded as a generalization of the maximum modulus theorem for matrix functions. The real rational subspace of $\mathcal{H}_\infty$ is denoted by $\mathcal{RH}_\infty$, which consists of all proper and real rational stable transfer matrices.

Let $G(s) \in \mathcal{RL}_\infty$ and recall that the $\mathcal{L}_\infty$ norm of a matrix rational transfer function G is defined as [16]

$$||G|||_\infty := \sup_w \bar{\sigma}[G(jw)] \tag{7.6}$$

The computation of the $\mathcal{L}_\infty$ norm of G is complicated and requires a search. A control engineering interpretation of the infinity norm of a scalar transfer function G is the distance in the complex plane from the origin to the farthest point on the Nyquist plot of G, and it also appears as the peak value on the Bode magnitude plot of $|G(jw)|$. Hence the ∞ norm of a transfer function can, in principle, be obtained graphically. To get an estimate, set up a fine grid of frequency points:

$$\{w_1, ..., w_N\} \tag{7.7}$$

Then, an estimate for $||G||_\infty$ is

$$\max_{1\le k\le N} \bar{\sigma}\{G(jw_k)\} \tag{7.8}$$

This value is usually read directly from a Bode singular value plot.

Bibliography

[1] M. C. Turner and D. J. Walker "Linear quadratic Bumpless transfer" *Control Systems Research, Department of Engineering, University of Leicester, Leicester LE1 7RH, UK. Automatica*, 36:1089-1101, 2000.

[2] S. Y. Cheong and M. G. Safonov "Bumpless Transfer for Adaptive Switching Controls". *Department of Electrical Engineering - Systems, University of Southern California, Los Angeles, CA. In IFAC World Congress*, 2008.

[3] K. Zheng, A. Lee, J. Bentsman and C. Taft. "Steady-state Bumpless Transfer under Controller Uncertainty Using the State/Output Feedback Topology" *43rd IEEE Conference on Decision and Control*, Dec 14-17, 2004. Atlantis, Paradise Island, Bahamas.

[4] K. Zheng, T. Basar, and J. Bentsman. "Steady-state Bumpless Transfer under Controller Uncertainty Using the State/Output Feedback Topology" *IEEE Transactions ON Automatic Control, VOL. 54, NO. 7*, July 2009

[5] I. Malloci, L. Hetel, J. Daafouz, C. Iung and R. Bonidal "$\mathcal{H}_\infty$ Bumpless Transfer Under Controller Uncertainty" *American Control Conference, ACC 2009, St Louis, Missouri*, 2009.

[6] M.C de Oliveira, J. C. Geromel and Bernussou. "An LMI optimization approach to multiobjective and robust $\mathcal{H}_\infty$ controller design for discrete time systems".

[7] A. Herrera, J. Vuelvas. "Control de Tensión en un Sistema de Transporte De Cintas Magnéticas", *Dept. Electrónica, Pontificia Universidad Javeriana, Bogotá D.C.*, 2009.

[8] T. L Vincent and W. J. Grantham *Nonlinear and Optimal Control Systems.*

[9] J. Vuelvas, J. Urrego. "Estimación y Control LPV para un Sistema de Transporte de Cintas Magnéticas", *Dept. Electrónica, Pontificia Universidad Javeriana, Bogotá D.C.*, 2010.

[10] YALMIP : A Toolbox for Modeling and Optimization in MATLAB. J. Lofberg. In Proceedings of the CACSD Conference, Taipei, Taiwan, 2004.

[11] A. Ladino "On Predictive Control for Hybrid Systems subject to Variable Time Delays". *Dept. Electrónica, Pontificia Universidad Javeriana, Bogotá D.C.*, 2012.

[12] J Bay. *Fundamentals of linear state space systems*. WCB/McGraw- Hill, Boston, 1999.

[13] L. Hetel. *Robust stability and control of switched linear systems*. PhD thesis, Nancy University, 2007.

[14] D. Liberzon. *Switching in Systems and Control*. Boston, Massachusetts, 2003.

[15] D. Patino. *Control of limit cycles in hybrid dynamical systems an introduction to cyclic switched systems : application to power converters*. Koln, lap, lambe edition, 2009.

[16] K. Zhou *Essentials of Robust Control*. Prentice Hall. May 25, 1999.

[17] M. Green and D. J. N. Limebeer. *Linear robust control*. New York: Prentice-Hall, 1995.

[18] R. Hanus, M. Kinnaert, and J.L Henrotte. "Conditioning technique, a general anti-windup and bumpless transfer method". Automatica, 23(6), 729-739. 1987.

[19] M. Safonov, E. Jonckheere, M. Verma, and D. Limebeer. "Synthesis of positive real multivariable feed-back systems". Int. J. Control, 45:817Ð842, 1987.